SAND2016-1898PE

ESR Experiments on a Single Donor in Silicon

L. A. Tracy, D. R. Luhman, S.M. Carr, J. Borchardt,
N.C. Bishop, G.A. Ten Eyck, T. Pluym, J. Wendt, W. Witzel,
R. Blume-Kohout, E. Nielsen, M.P. Lilly, M.S. Carroll

Sandia National Laboratories

This work was performed, in part, at the Center for Integrated Nanotechnologies, a U.S. DOE, Office of Basic Energy Sciences user facility. This work was supported by the Laboratory Directed Research and Development program at Sandia National Laboratories. Sandia National Laboratories is a multi-program laboratory managed and operated by Sandia Corporation, a wholly owned subsidiary of Lockheed Martin Corporation, for the U.S. Department of Energy's National Nuclear Security Administration under contract DE-AC04-94AL85000.

Semiconductor spin qubits

coupled quantum dots

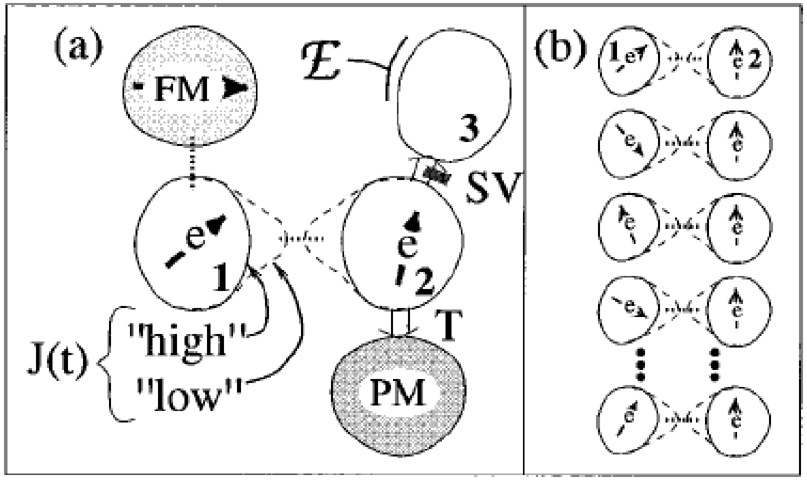

D. Loss and D. P. DiVincenzo,
Phys. Rev. A **57**, 120 (1998)

donor nuclear spin qubits

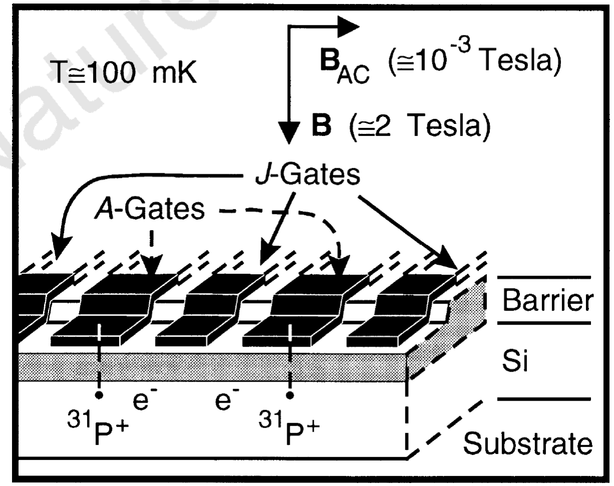

B. E. Kane, Nature **393**, 133 (1998)

donor electron spin qubits

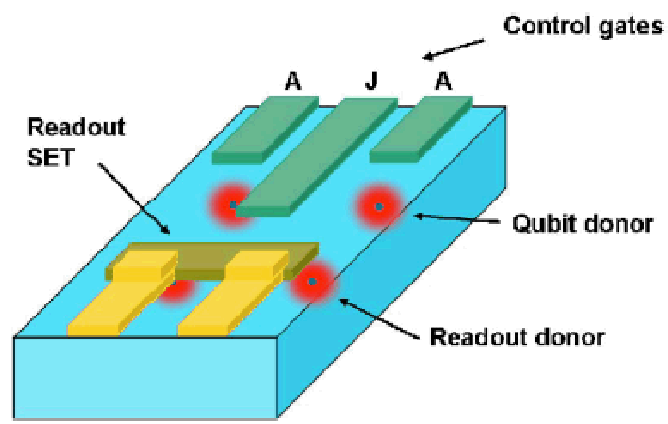

C. D. Hill *et al.*, Phys. Rev. B **72**, 045350 (2005)

DiVincenzo criteria:

- identification of well-defined qubits
- reliable state preparation
- low decoherence
- accurate quantum gate operations
- strong quantum measurements

GaAs quantum dot spin qubits

coherent single spin oscillations

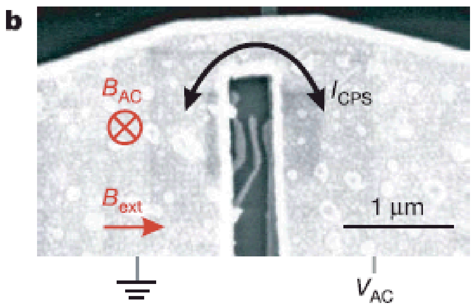

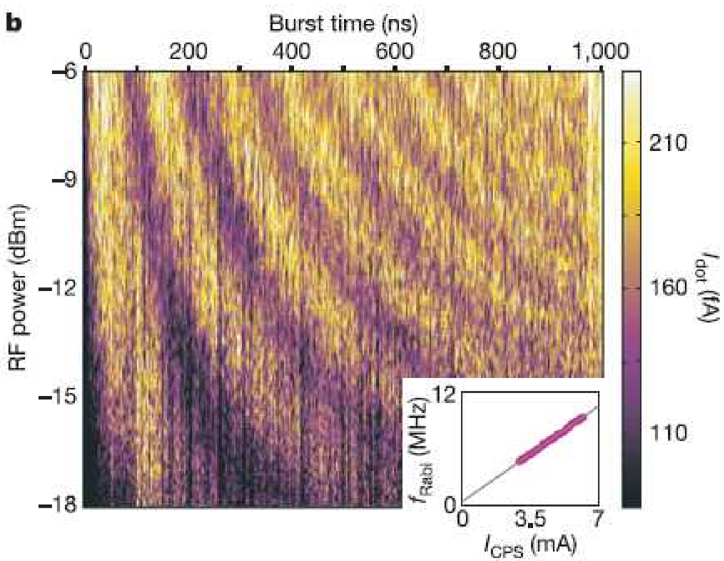

F. H. L. Koppens *et al.*, Nature **442**, 766 (2006)

singlet-triplet qubit

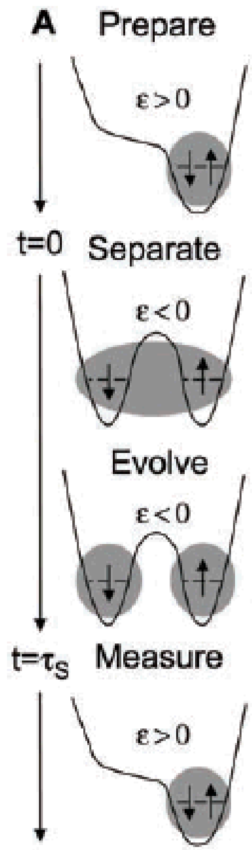

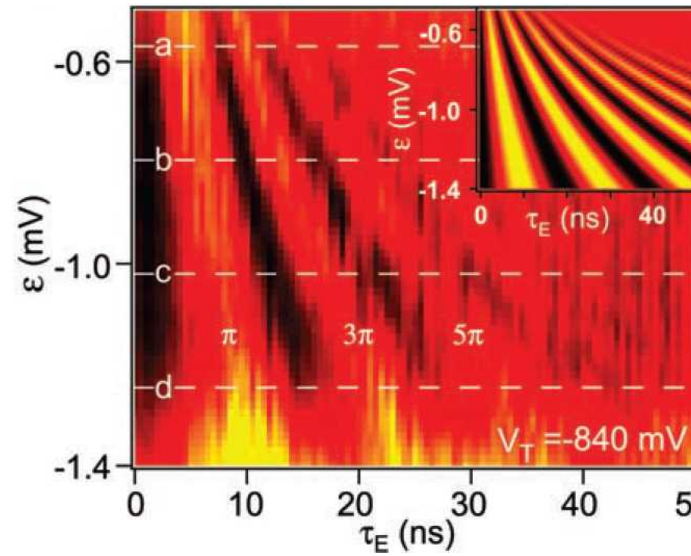

J. R. Petta *et al.*, Science **442**, 766 (2005)

Nuclear spins

Nuclear spins in GaAs

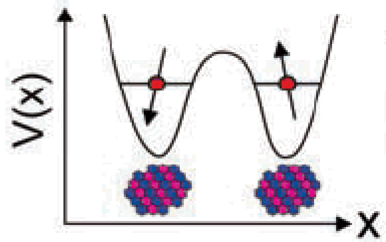

GaAs:
$T_2^* \sim 10$ ns

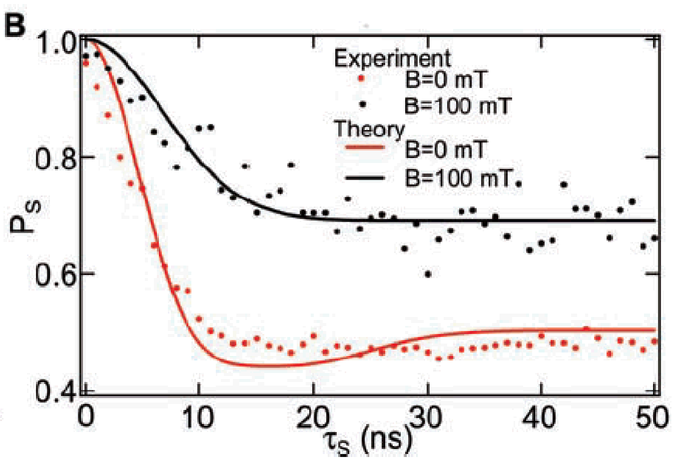

J. R. Petta *et al.*, Science **442**, 766 (2005)

$T_2^{GPMG} \sim 200$ μs

H. Bluhm *et al.*, Nature **7**, 109 (2011)

T_2 in bulk P doped ^{28}Si

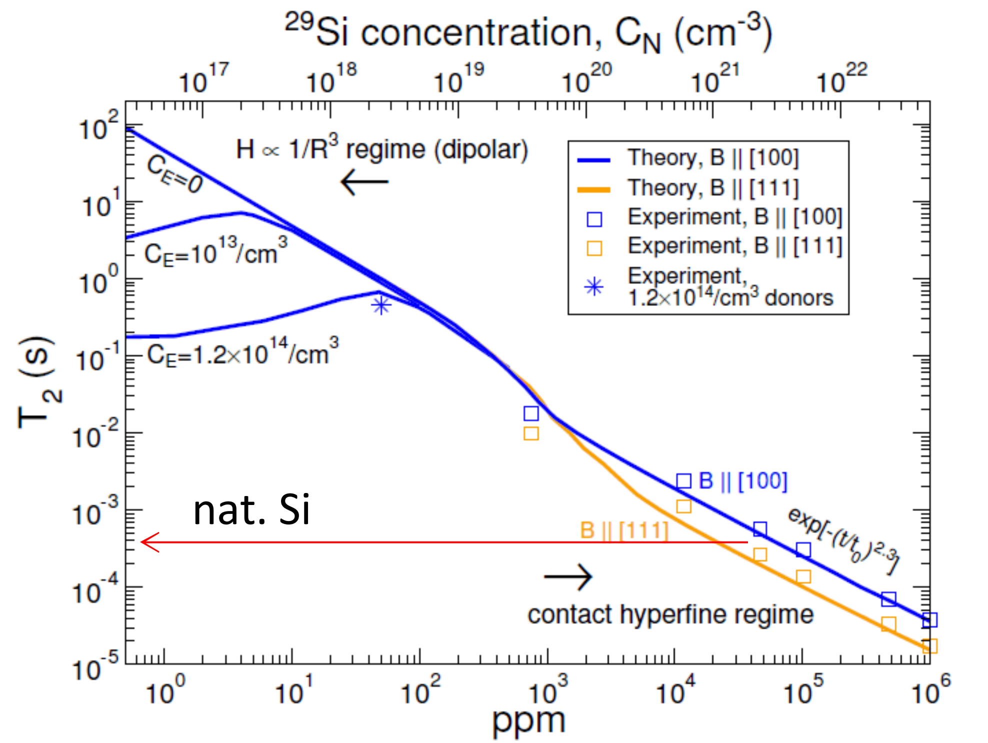

W. Witzel *et al.*, Phys. Rev. Lett. **105**, 187602 (2010)
E. Abe *et al.*, Phys. Rev. B **82**, 121201R (2010)
A. M. Tyryshkin *et al.*, Nat. Mat. **11**, 143 (2012)

Silicon spin qubits

SiGe quantum dot

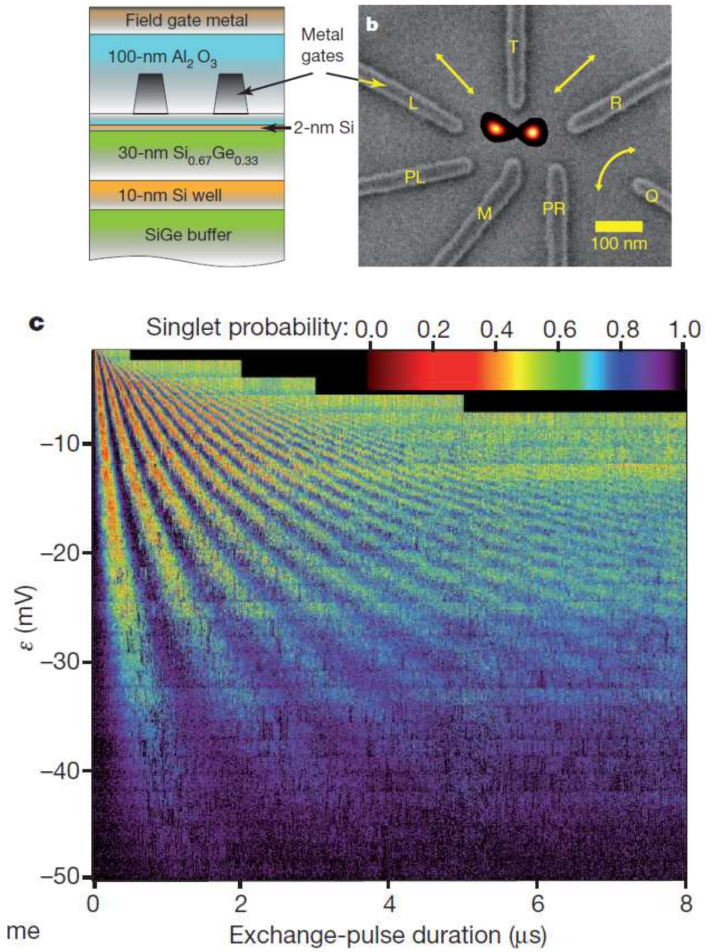

$T_2^* = 360$ ns

B. M. Maune *et al.*, Nature **481**, 344 (2012)

Donor qubit

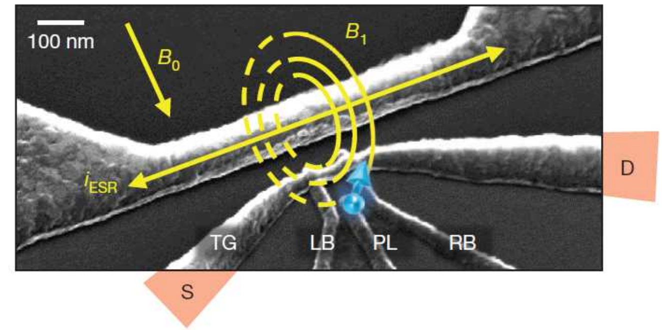

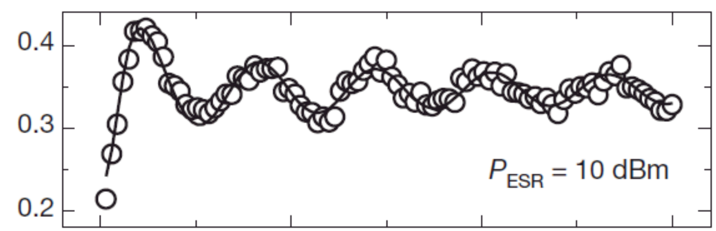

$T_2^* = 55$ ns

$T_2^{echo} = 200$ μs

J. Pla *et al.*, Nature **489**, 541 (2012)

Sandia National Laboratories

Enriched ^{28}Si devices

SiGe triple dot

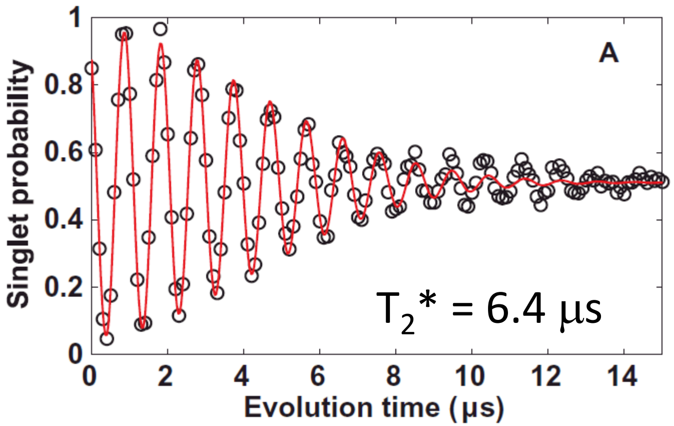

K. Eng *et al.*, Sci. Adv. (2015)

Si MOS quantum dot

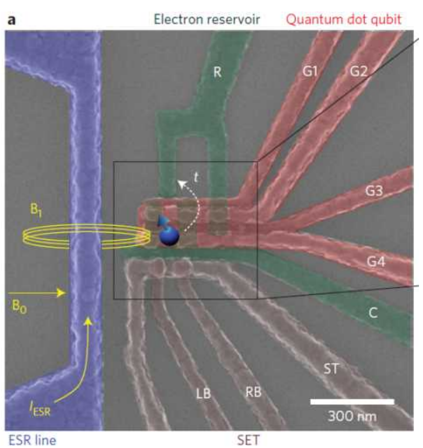

$T_2^* = 120\ \mu s$
$T_2^H = 1.2$ ms

M. Veldhorst *et al.*, Nature Nanotech. **9**, 981 (2014)

Single donor qubit

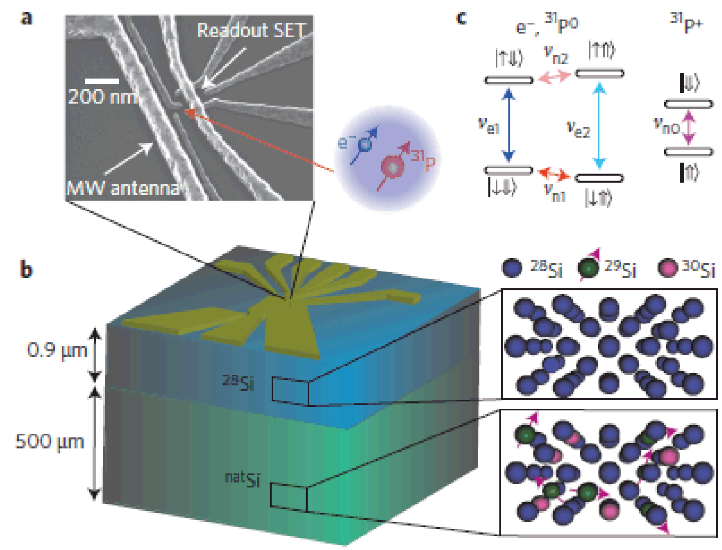

$T_2^* = 270\ \mu s$
$T_2^H = 0.95$ ms

J. T. Muhonen *et al.*, Nat. Nanotech. **9**, 986 (2014)

Sandia National Laboratories

Outline

- Device fabrication
- Single spin readout and initialization
- Natural silicon qubit
- Enriched silicon 28 qubit

Si donor qubit fabrication – SNL Si foundry

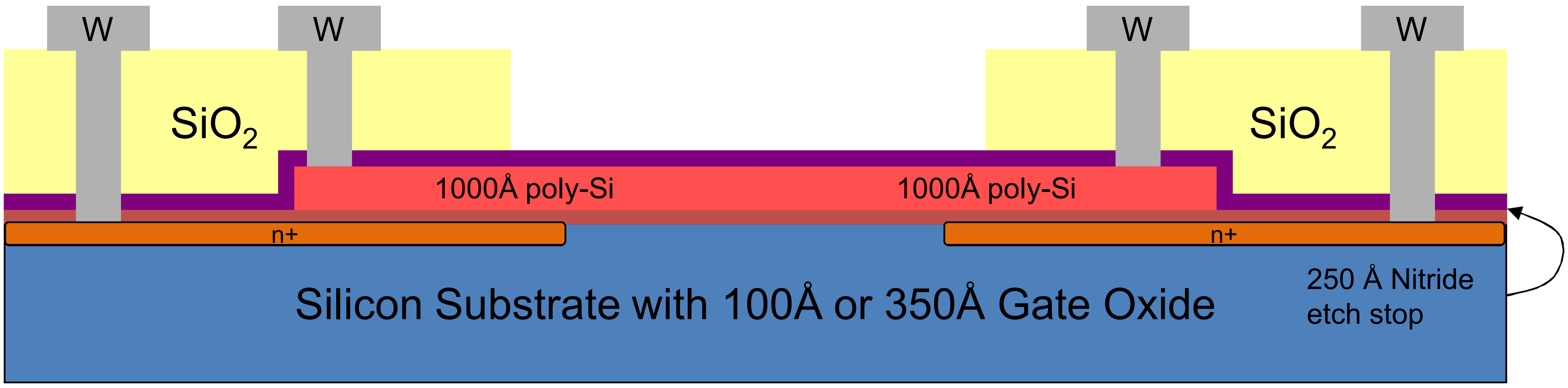

<u>**MOS Stack from Si fab**</u>

Many electron QDs possible with 0.18 μm litho

Structures fabricated for external community (NIST, LBNL, CQC2T, U. Princeton)

7,500 – 15,000 4K mobility

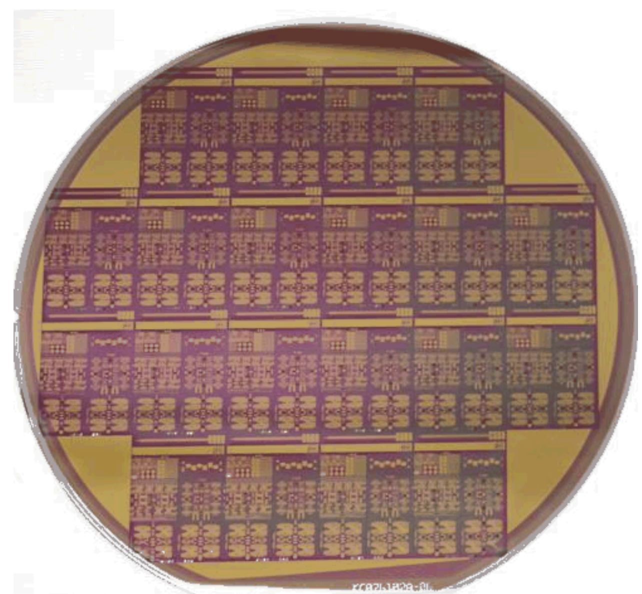

T. Pluym, G. A. Ten Eyck, N. Bishop,

Nanostructure fabrication

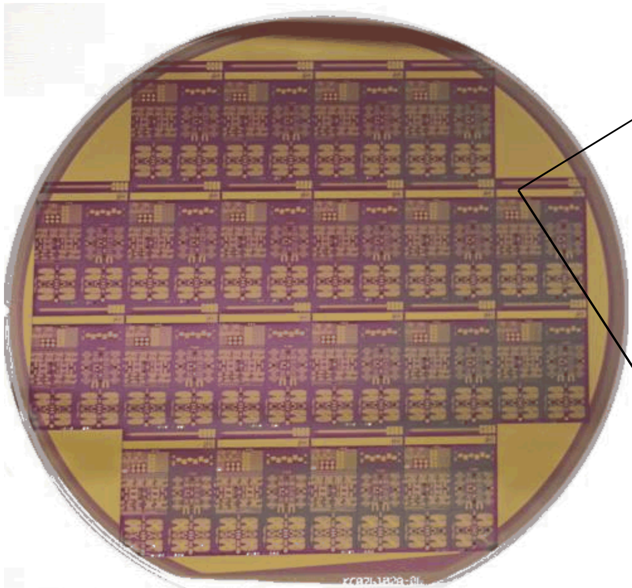

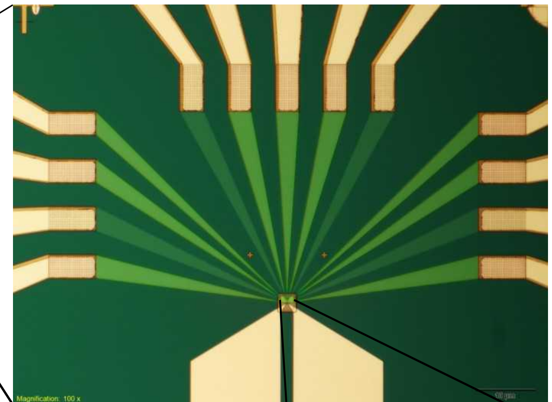

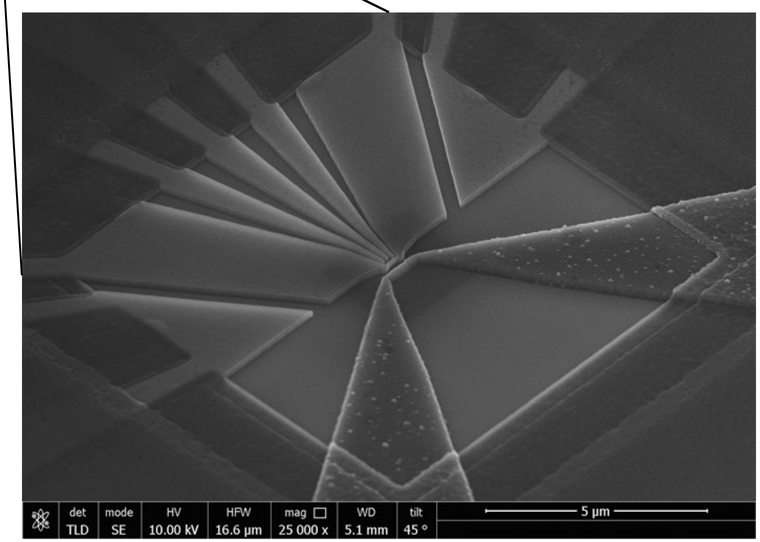

EBL and poly etch to define nanostructure gates

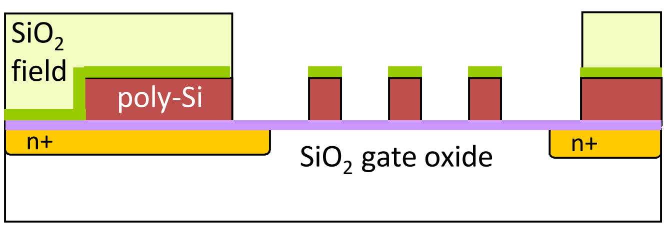

G. A. Ten Eyck, J. R. Wendt, J. Dominguez, B. Silva, N. Bishop,

Sandia National Laboratories

Donor electron spin readout device

- Polysilicon gates used to form single electron transistor (SET) at Si/SiO_2 interface
- Timed implant with PMMA window, self-aligned with polysilicon gates
- Implant range ~28 - 15 nm below SiO_2/Si interface, ~18 - 44 nm straggle (Sb@120 keV vs. P@45 keV)
- $4x10^{11}/cm^2$ dose → ~15 donors in 60 x 60 nm^2 window

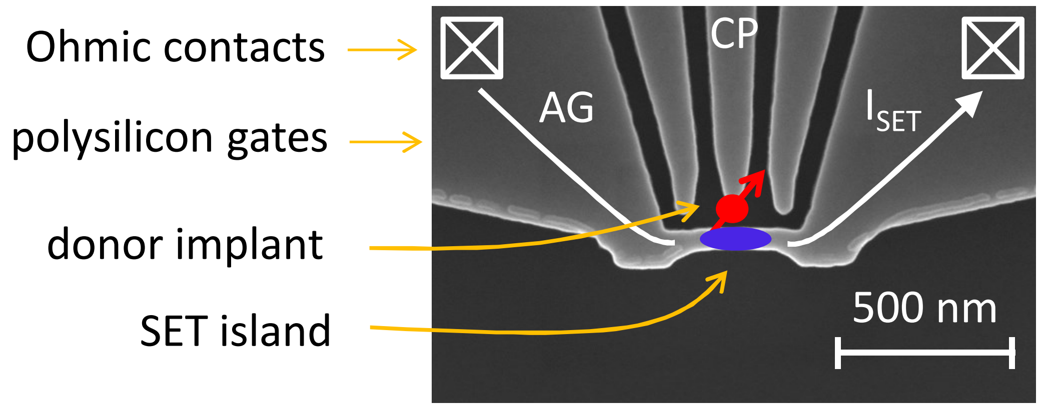

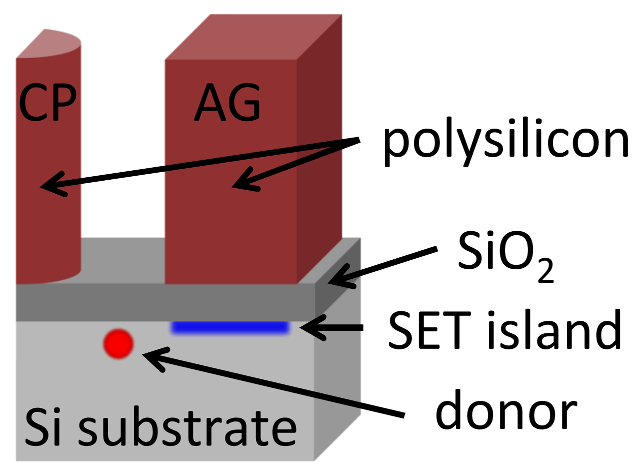

Transport through SET

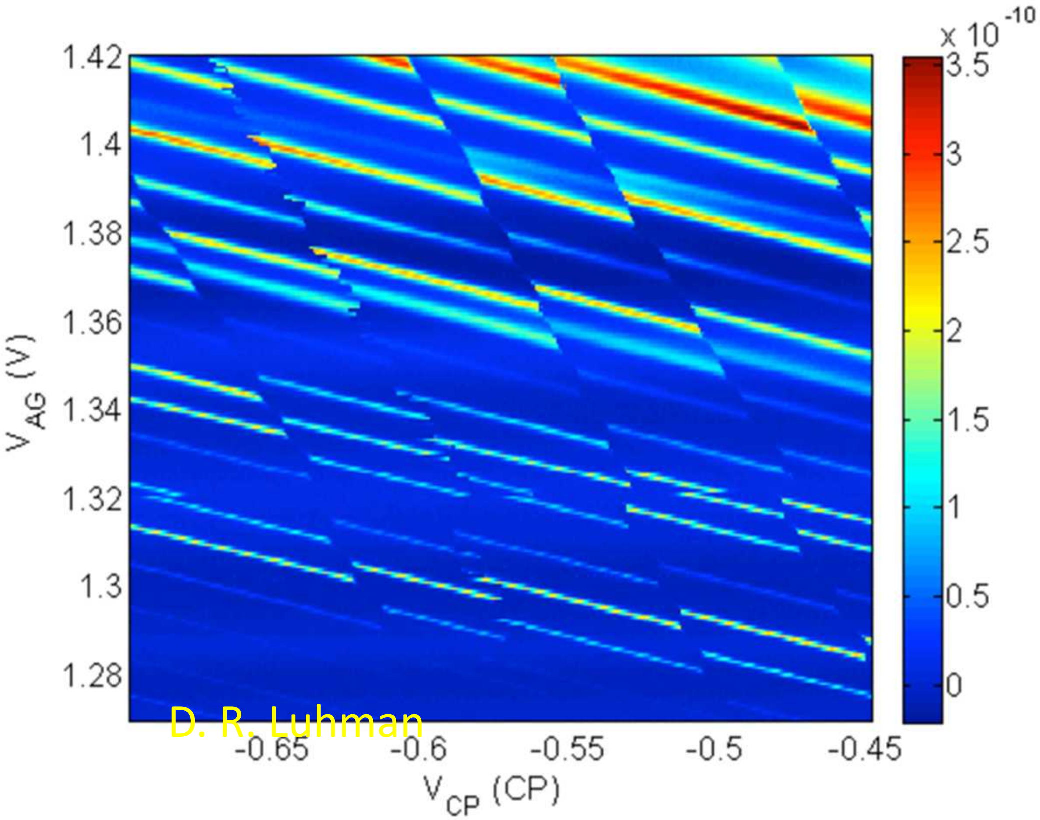

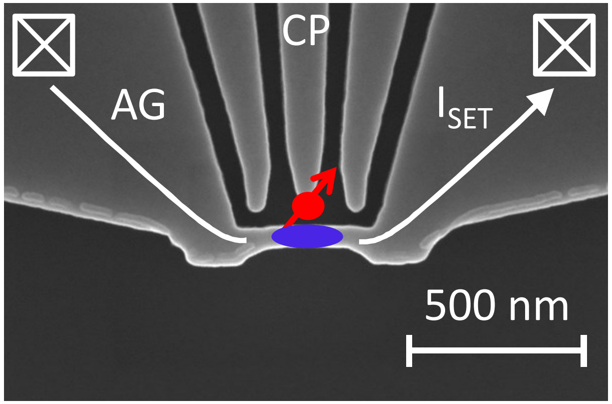

Coulomb blockade in quantum dot

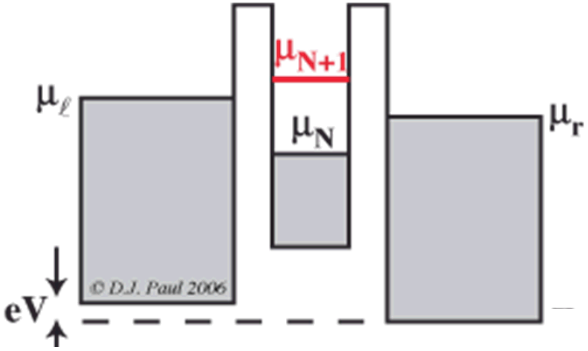

Coulomb blockade in SET has discontinuities due to donor charge transitions (donor electron tunneling to SET island)

Single spin readout

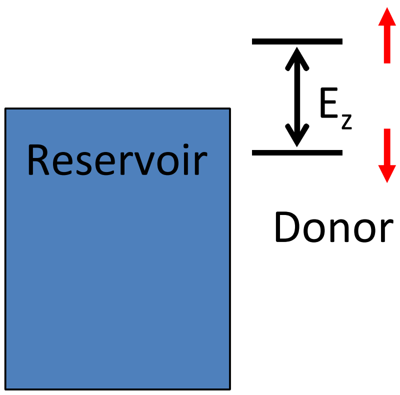

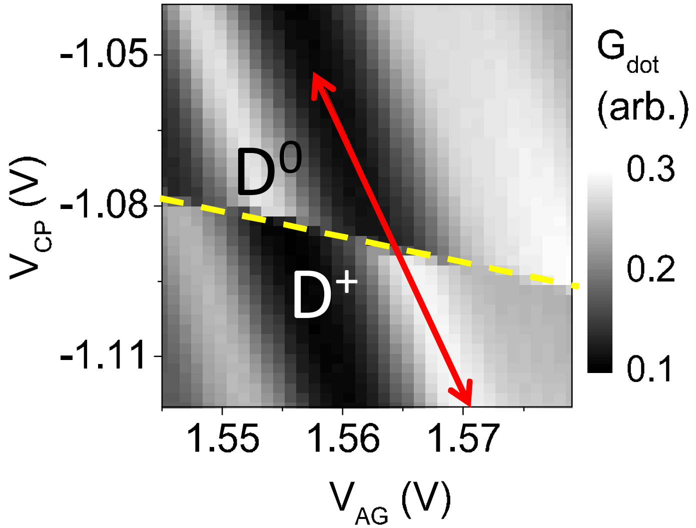

- Spin selective tunneling from donor to reservoir in magnetic field
- Used to initialize and read spin
- B = 1.3 T → E_z ~ 1.7 K

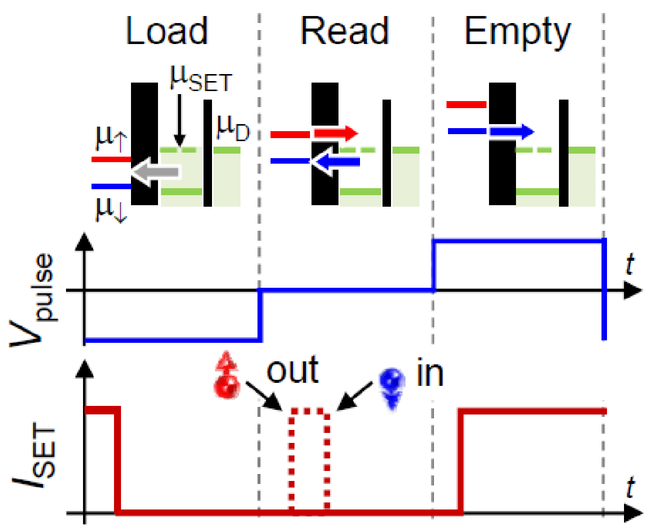

J. M. Elzermann *et al.*, Nature **430**, 431 (2004)
A. Morello *et al.*, Nature **467**, 687 (2010)

Sandia National Laboratories

Tuning read level

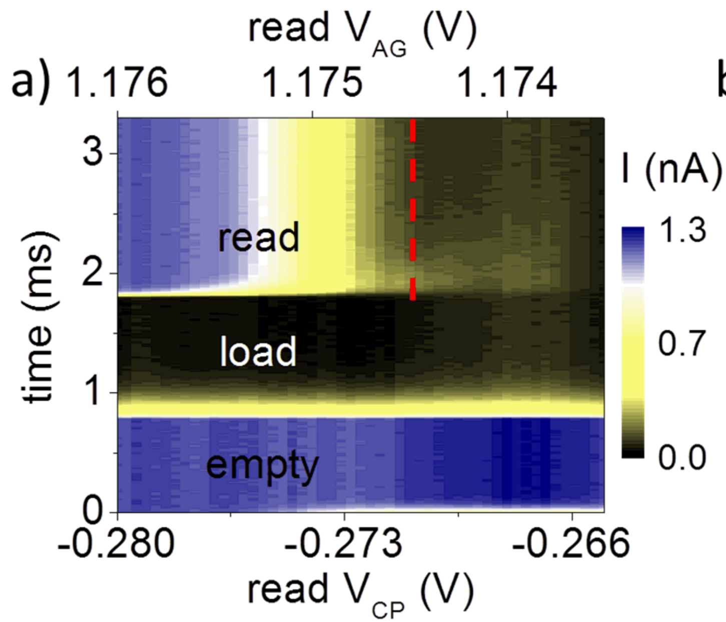

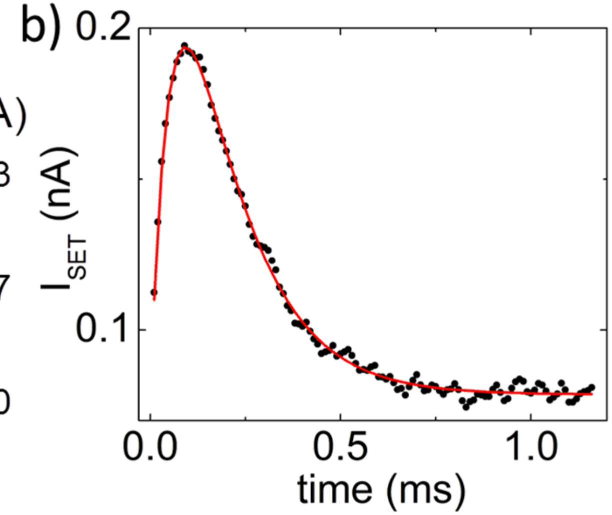

$$\Gamma_{\downarrow l} = 15.1 \pm 0.7\ \mathrm{kHz}$$
$$\Gamma_{\uparrow u} = 6.8 \pm 0.2\ \mathrm{kHz}$$

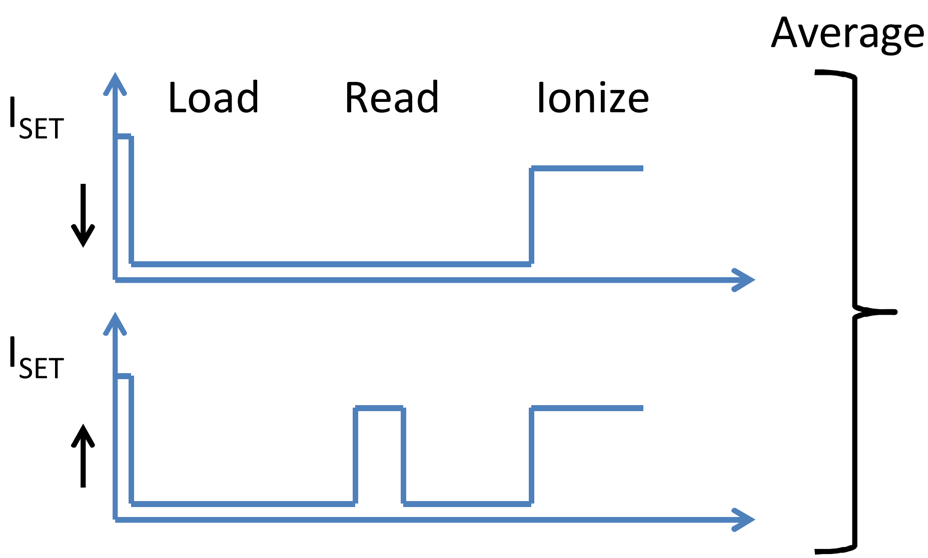

BW for high fidelity single shot readout?

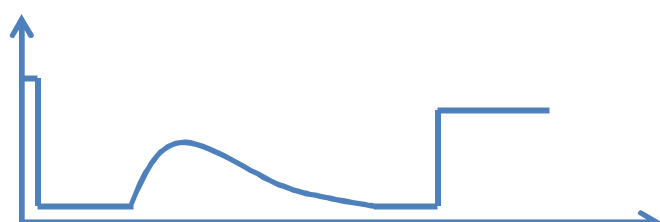

averaged readout

RF Reflectometry

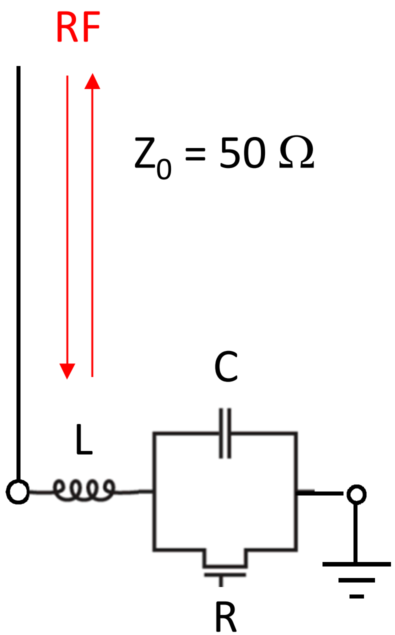

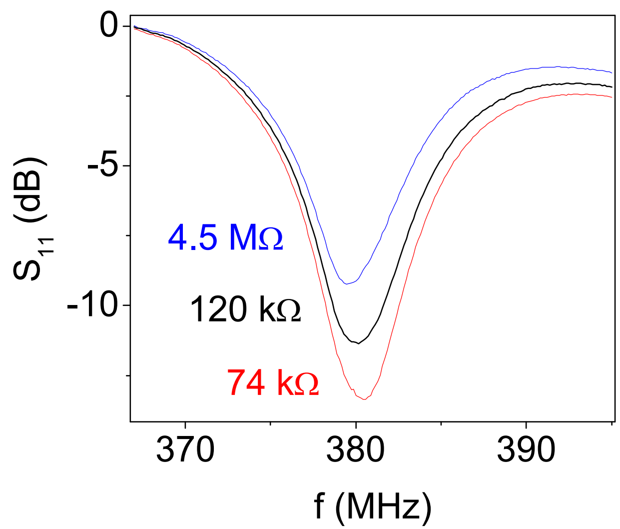

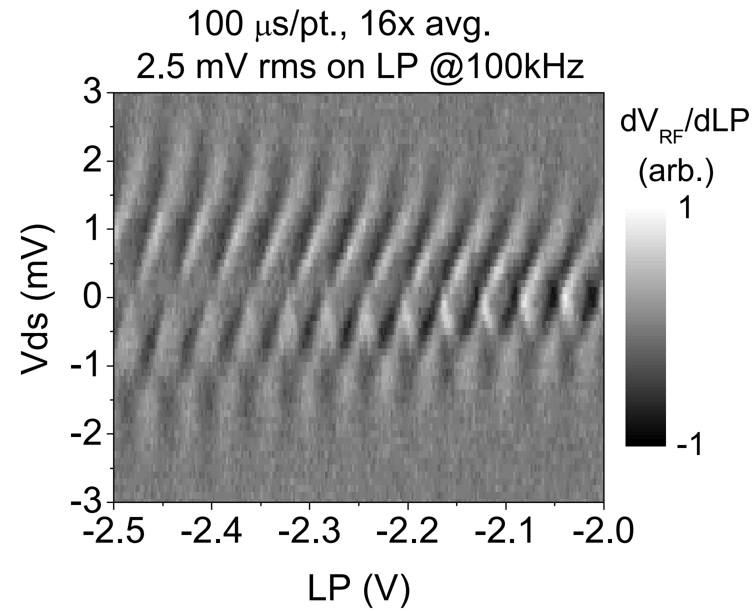

- Si MOS RF SET: 10 MHz BW and ~10^{-9} Ω^{-1} /√Hz sensitivity and for Vsd ~ 200 μV
- Corresponds to noise ~200 fA $Hz^{-1/2}$
- Other groups have achieved ~100 fA $Hz^{-1/2}$ (Reilley *et al.*, Phys. Rev. Lett. (2007)

Schoelkopf et al., Science 1998

Sandia National Laboratories

Read-out circuit with amplification at sample

Si chip

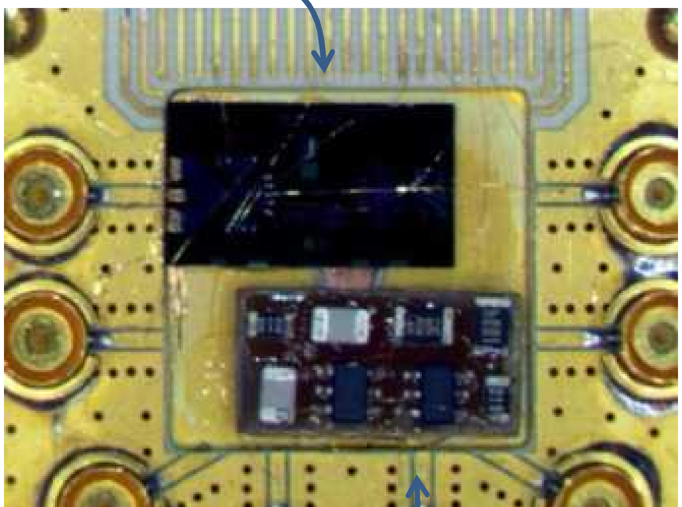

HEMT circuit

- Commercial InGaAs enhancement mode HEMTs

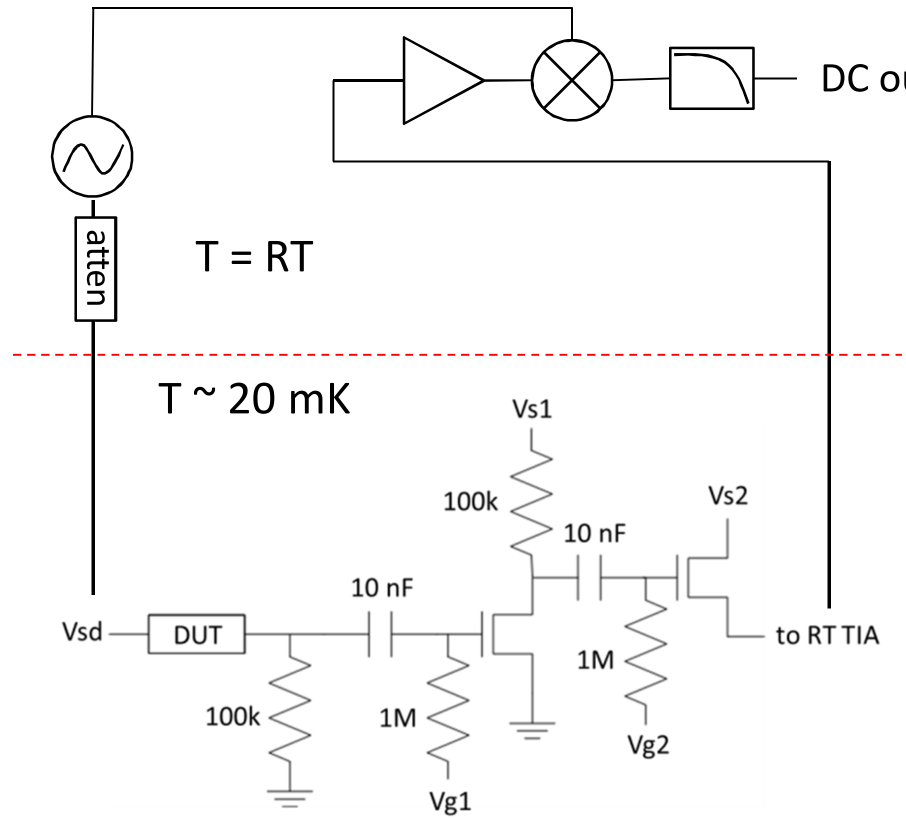

Sandia National Laboratories

Gain and bandwidth

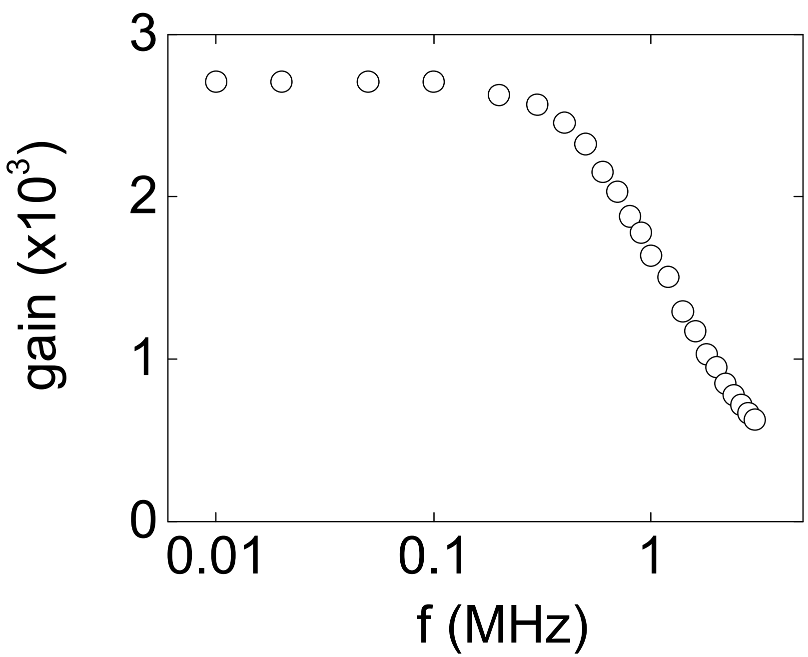

- DUT = 100k resistor
- Meas BW ~ 1.3 MHz
- 1st HEMT: 3 μW, 2nd HEMT 10 μW
  → 13 μW total
- tradeoff gain for power?

Quantum Information S&T

Noise

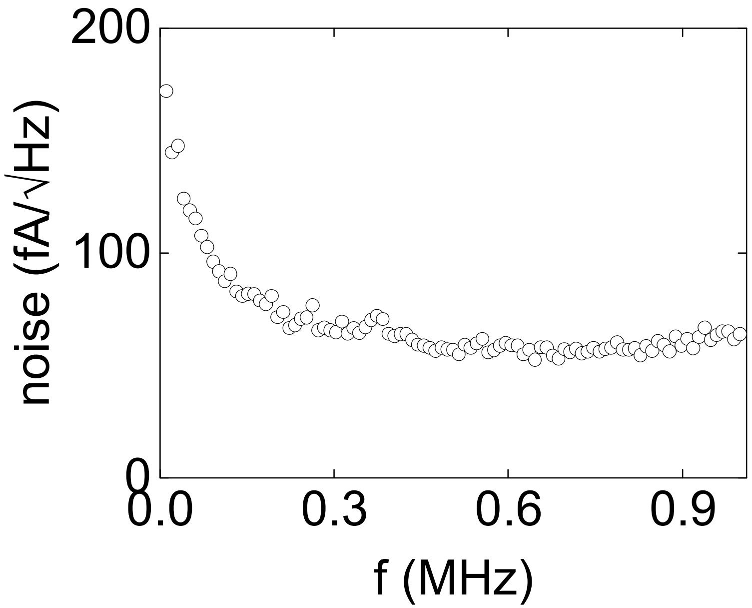

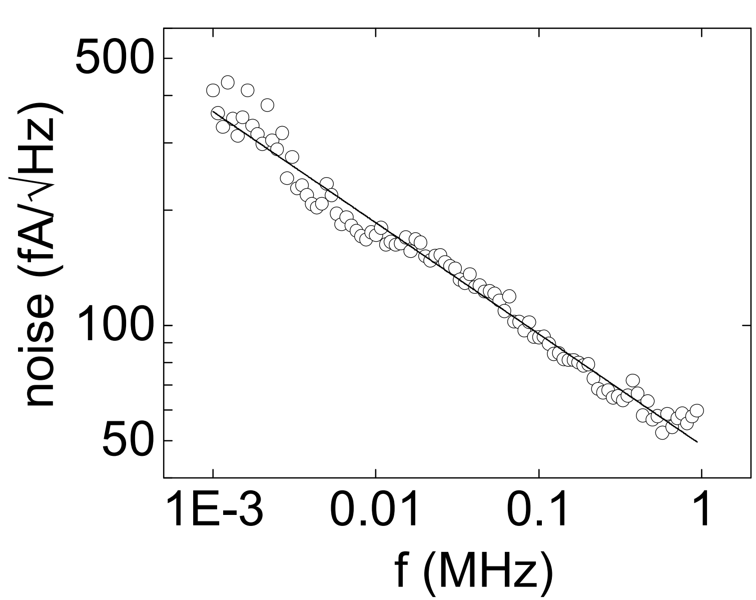

- ~ 70 fA $Hz^{-1/2}$ above 0.3 MHz
- 1/f noise (~ $f^{-0.3}$)

Sandia National Laboratories

Temperature

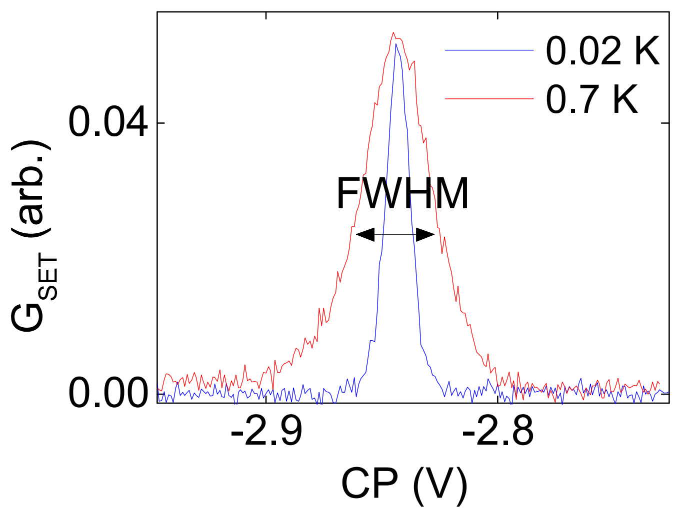

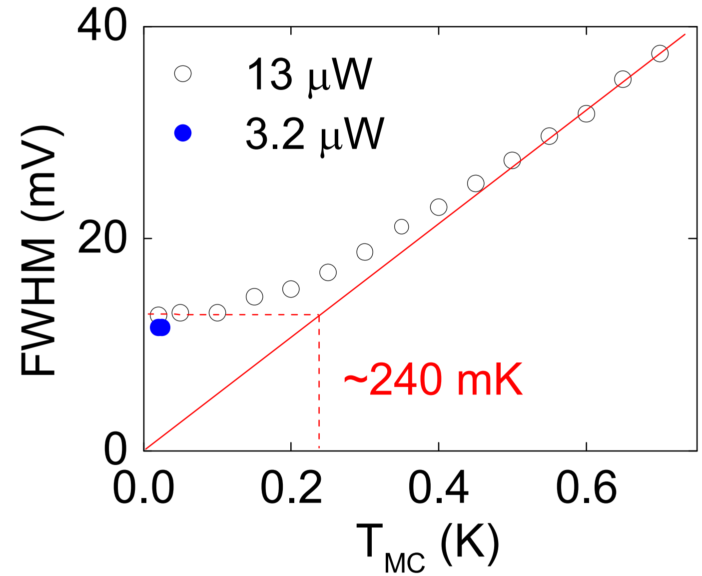

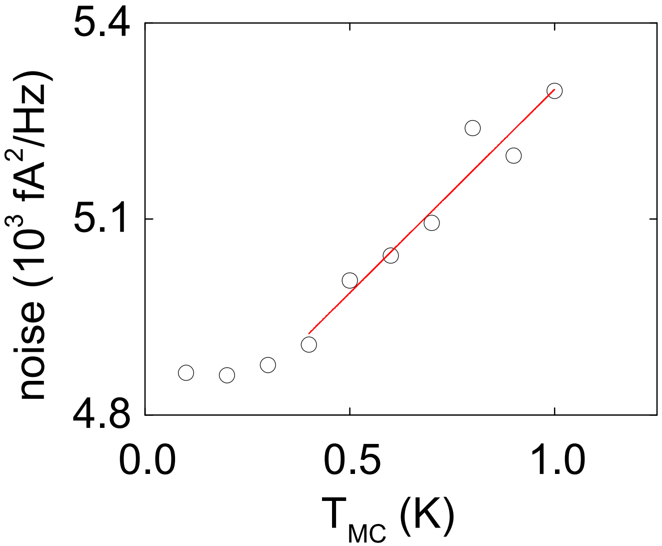

- SET temperature ~ 240 mK at 13 μW
- ~220 mK at 3 μW suggests not dominated by HEMT
- Slope of noise vs. T_{MC} greater than expected for simple Johnson noise
- Knee of noise vs. T_{MC} suggests 1st HEMT ~ 300 mK

Sandia National Laboratories

Quantum Information S&T

Live SET tuning

- Rapid search for donor charge transitions
- Response rate of offset gives tunnel time estimate

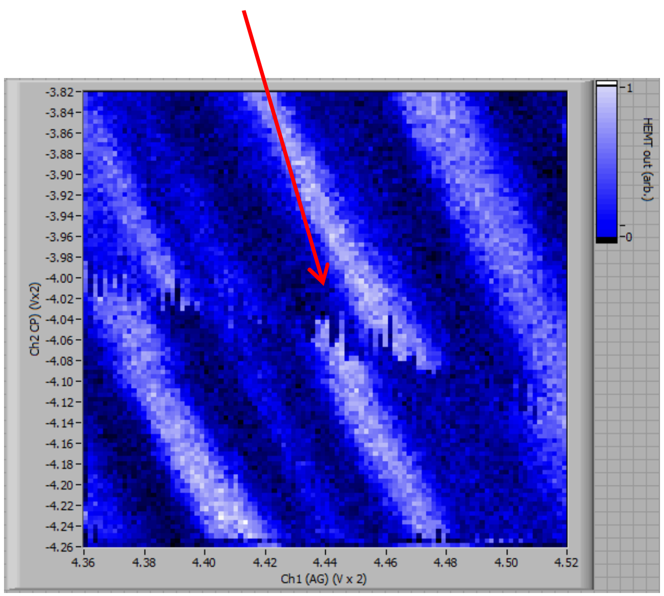

100 x 100 scan, ~3 Hz refresh rate

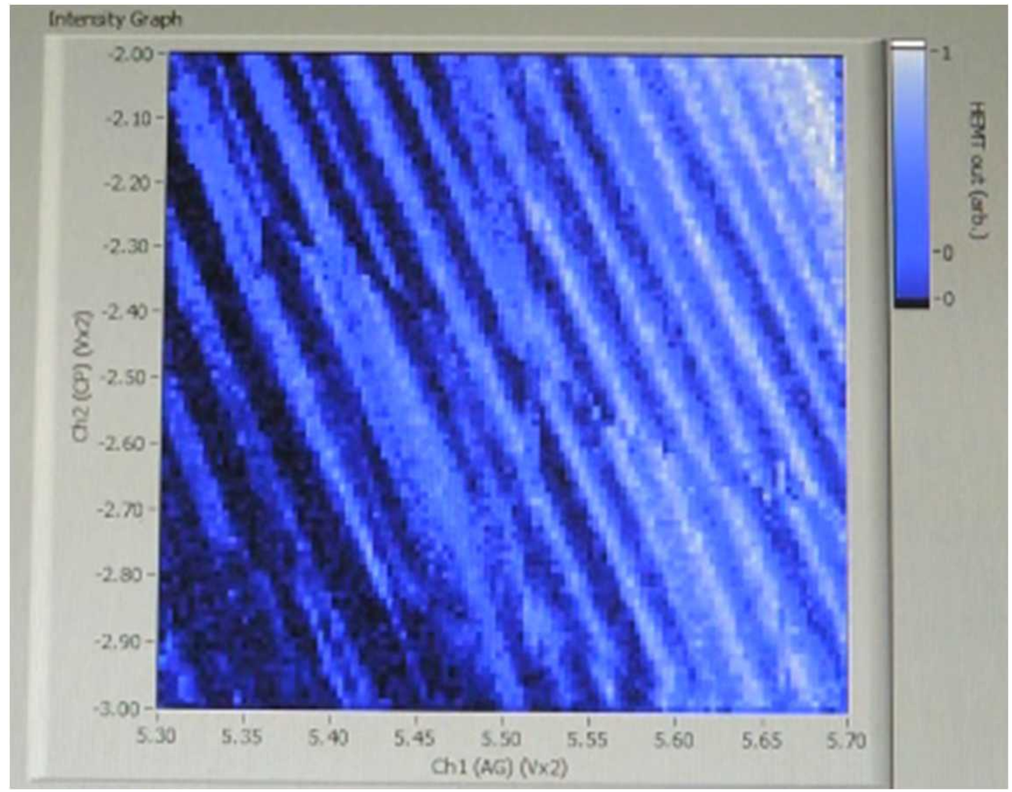

Single shot spin readout

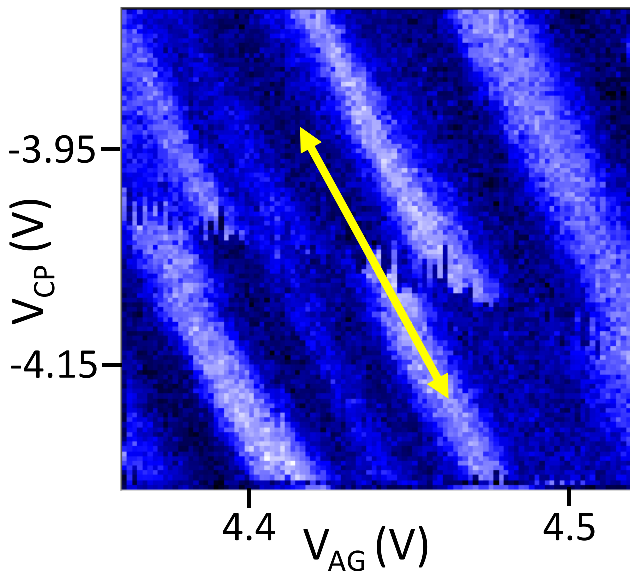

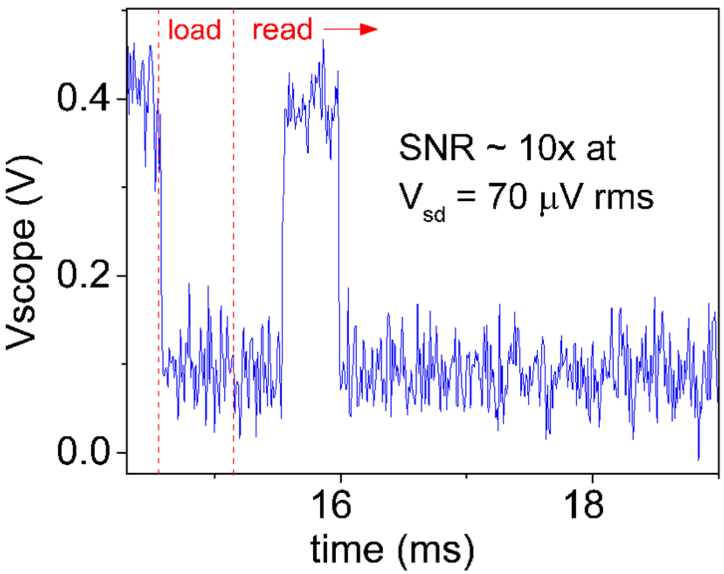

- Single shot event SNR ~ 10x for Vsd = 70 uV rms
- Effect of dry fridge triboelectric noise reduced by gain before coax and by working at higher frequencies

Magnetic field dependence of T_1 (Sb donor)

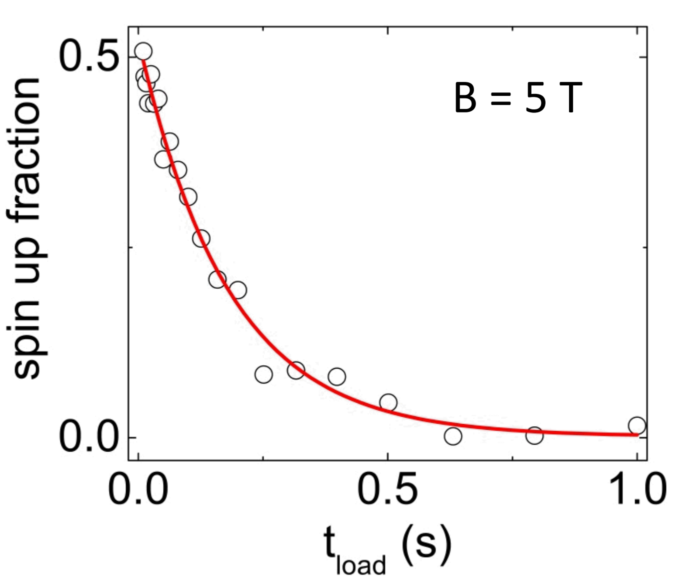

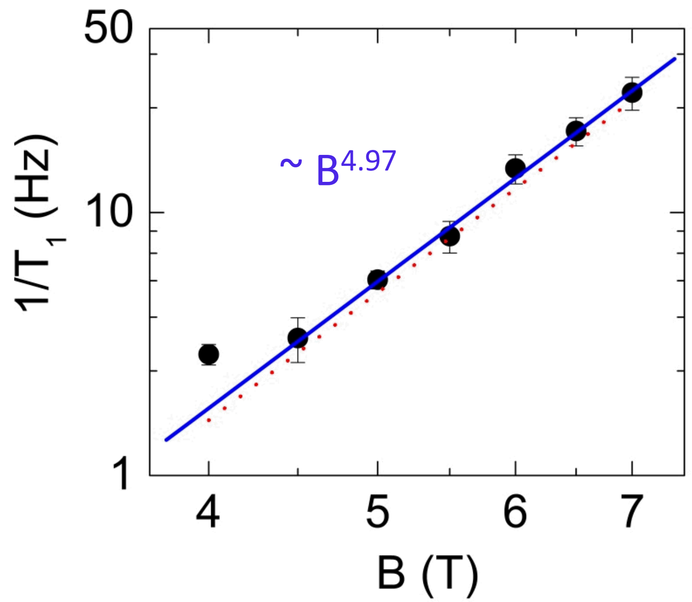

- Expect $T_1 \sim B^5$ for donor spins, due to g-factor dependence on strain (L. Roth, Phys. Rev. (1960), H. Hasegawa, Phys. Rev. (1960))
- Red dotted line expected T_1 extrapolated from bulk ESR meas (D. K. Wilson and G. Feher, Phys. Rev. (1961))
- T_1 ~ 350 ms at low fields, may be due to dipolar interactions with neighboring Sb electron spins (~$10^{17}/cm^3$) (Morello *et al.*, Nature (2010))
- $T_1 \geq 350$ ms at B = 1.3 T

Tracy *et al.*, Appl. Phys. Lett. (2013)

Quantum Information S&T

Sandia National Laboratories

Local ESR & NMR

- Can use local RF and microwave magnetic fields to manipulate electron or nuclear spin on a quantum dot or donor
- Extract T_2, perform single qubit operations

ESR with GaAs quantum dot

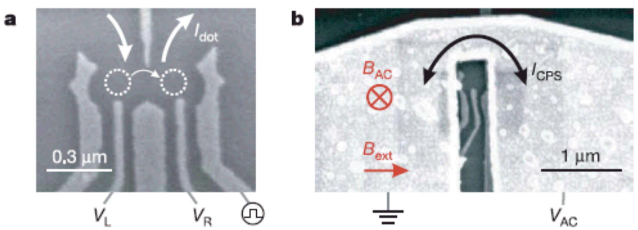

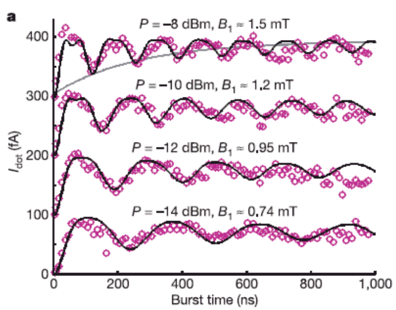

F. H. L. Koppens et al., Nature (2006)

ESR & NMR with single donor in Si

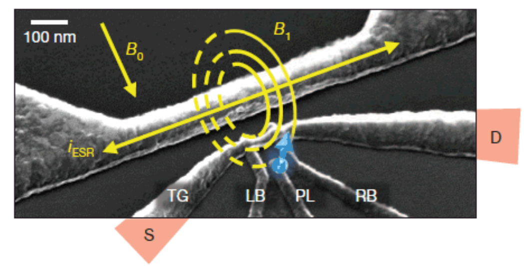

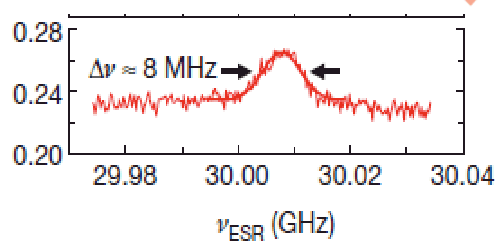

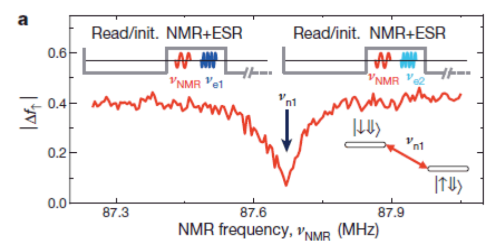

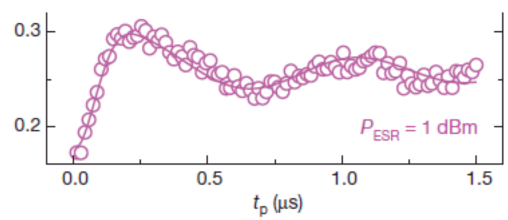

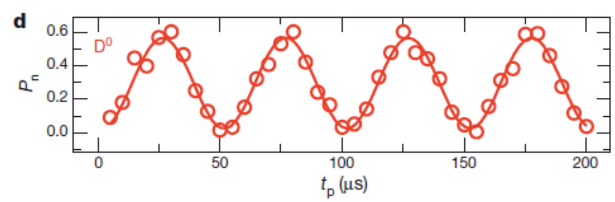

J. Pla et al., Nature (2012)

J. J. Pla et al., Nature (2013).

Electron spin resonance with P donor in Si

Zeeman splitting

<u>For electron:</u>

$E_Z = g\ \mu_B\ B_{z,}\ g = -1.9985$

At 1 Tesla

$E_Z = 1.34$ K = 28 GHz

<u>For nuclear spin:</u>

At 1 Tesla

$E_Z = 0.8$ mK = 17.2 MHz

With hyperfine coupling

$$H = \gamma_e B_0 S_z - \gamma_N B_0 I_z + A S \cdot I$$

A = 117 MHz for P

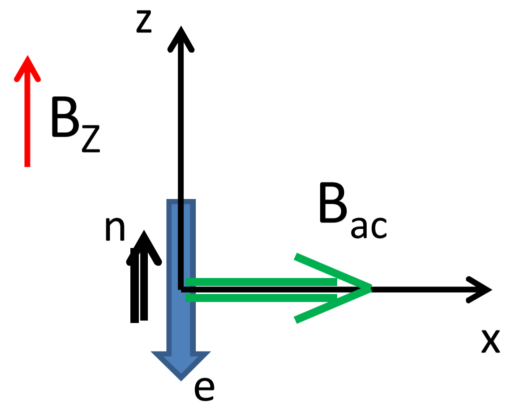

ESR transitions

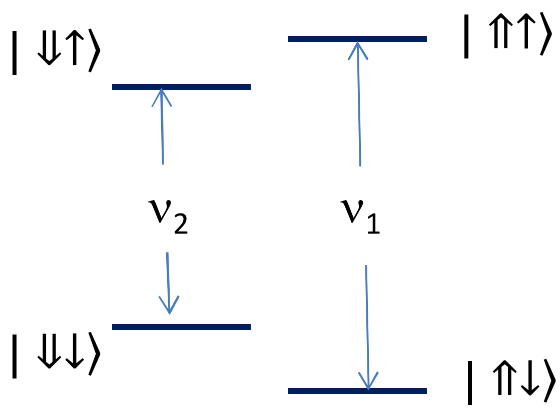

Coherence times T_2*, T_2

Larmor precession

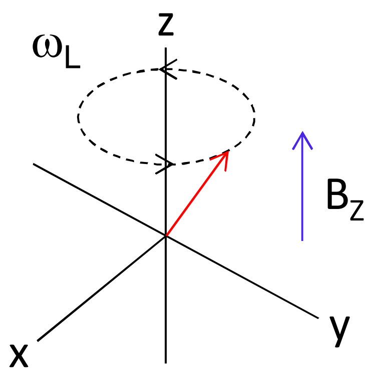

Rotating frame

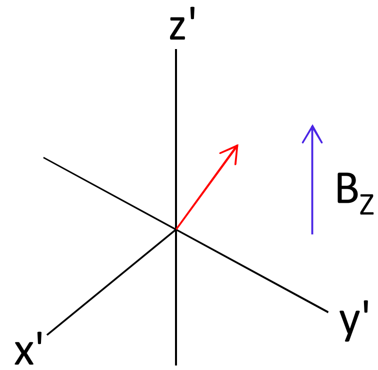

Rabi oscillations

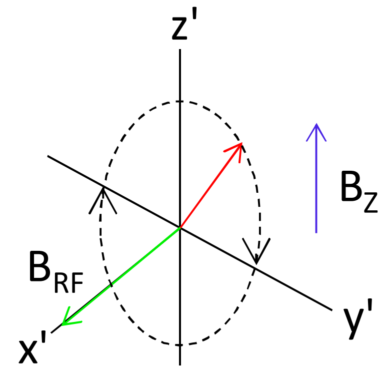

T_2* dephasing

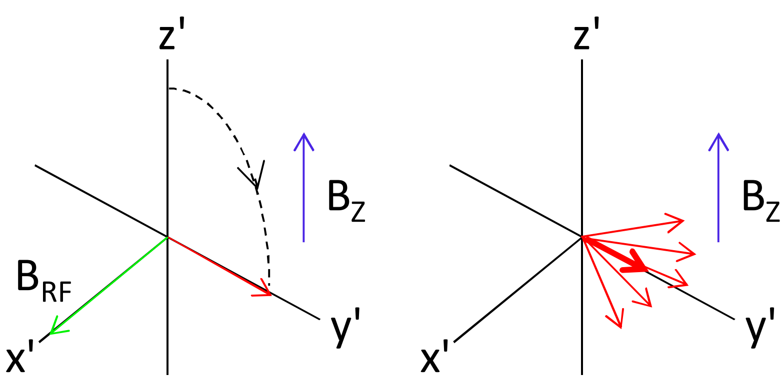

π/2 pulse

Hahn echo T_2 meas

for echo
wait τ ...

wait τ ...
(refocus)

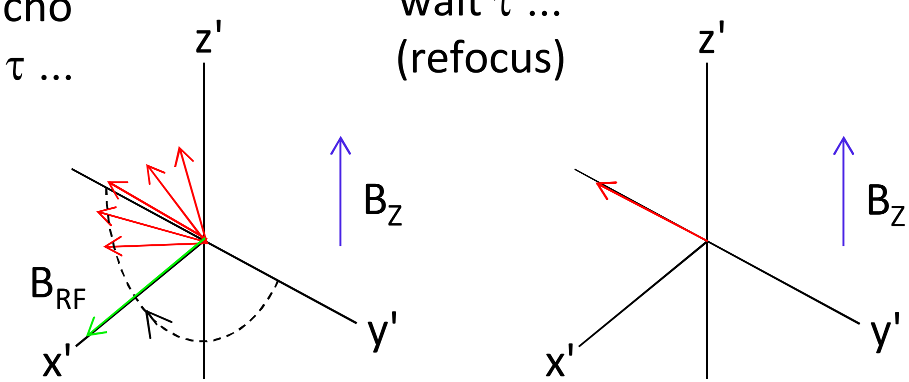

π pulse

local ESR device

- Timed P implant with PMMA window, self-aligned with polysilicon gates
- 45 keV implant, range ~15 nm below SiO_2/Si interface
- 4 – 8 $\times 10^{11}$/cm^{-2} dose → ~ 40 - 80 P donors in 100 x 100 nm^2 window
- Nearby microwave antenna for local ESR
- Dry dilution refrigerator
  - T_{base} = 10 - 20 mK
  - $T_{electron}$ = 200 - 300 mK

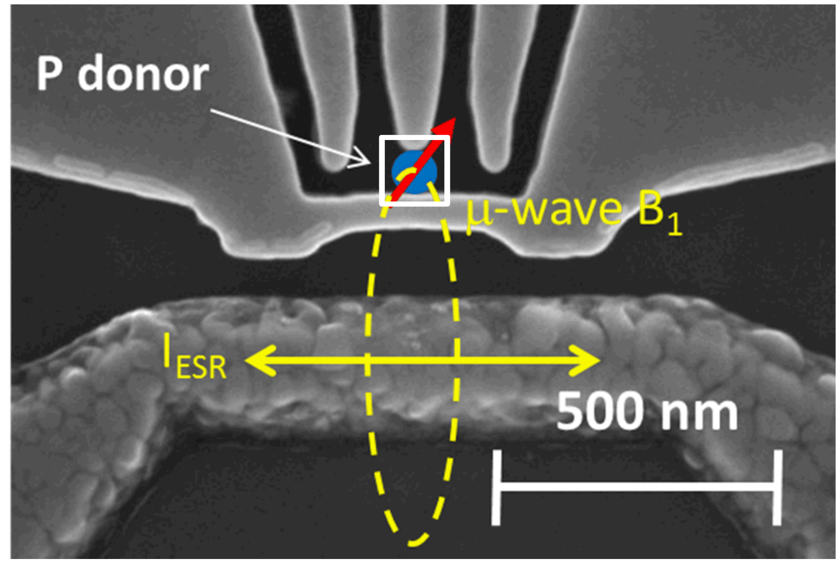

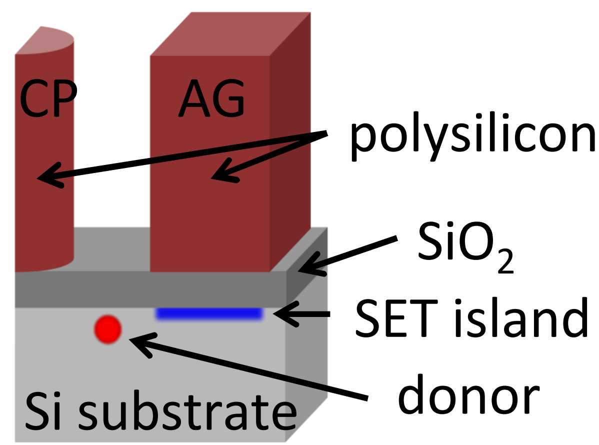

Sandia National Laboratories

Natural Si device - Rabi Oscillations

D. R. Luhman

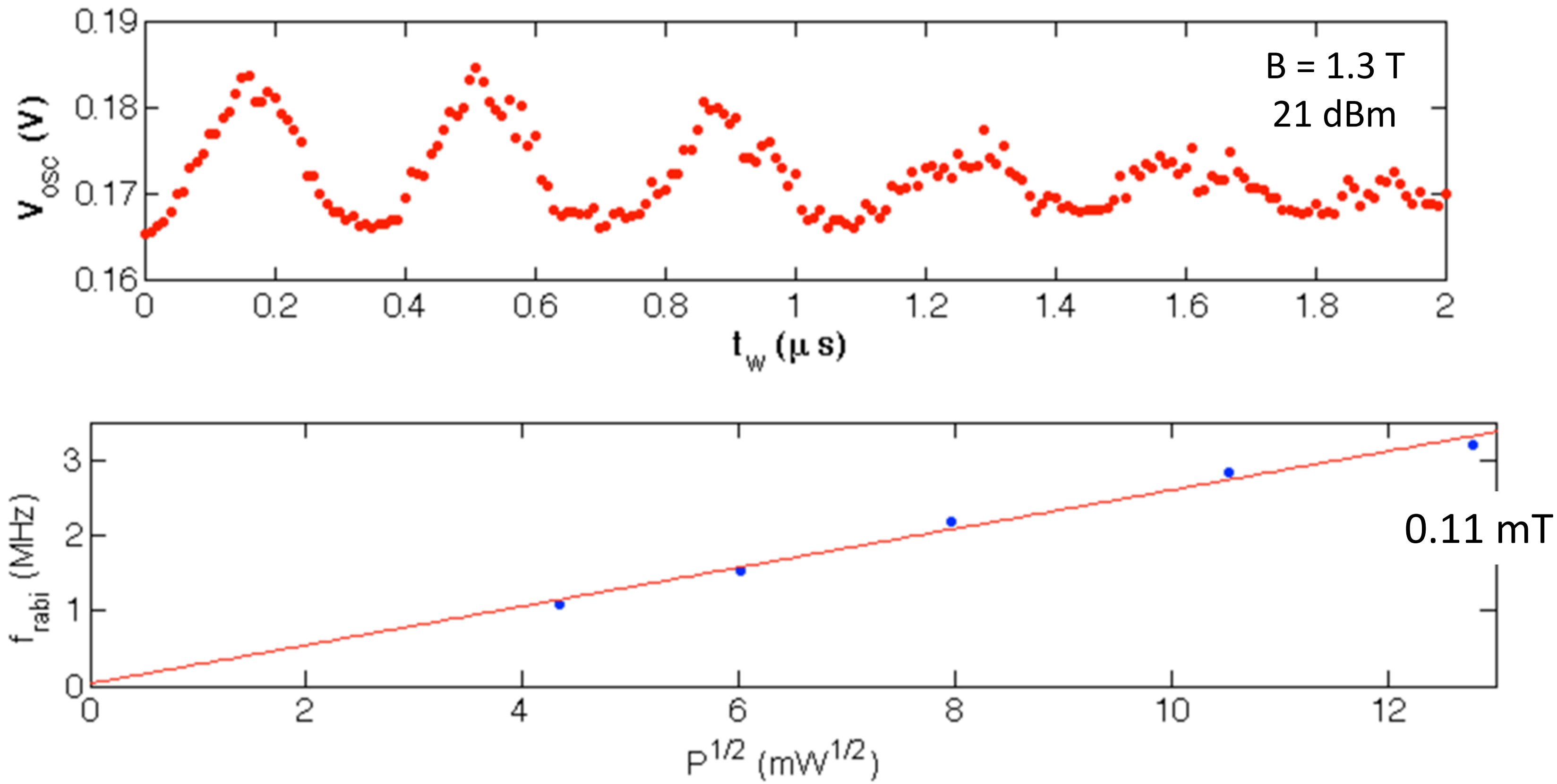

- Pre-HEMT implementation, dry fridge noise prevents single shot spin meas
- f_{B1} ~ 36 GHz @ B = 1.3 T
- Rabi frequency linear in B_1

T_2^* Measurement

D. R. Luhman

Spin echo technique:
Vary τ_2 relative to $\tau_1 = 10\ \mu s$

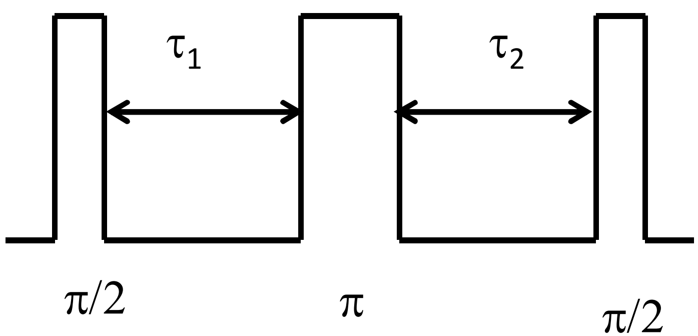

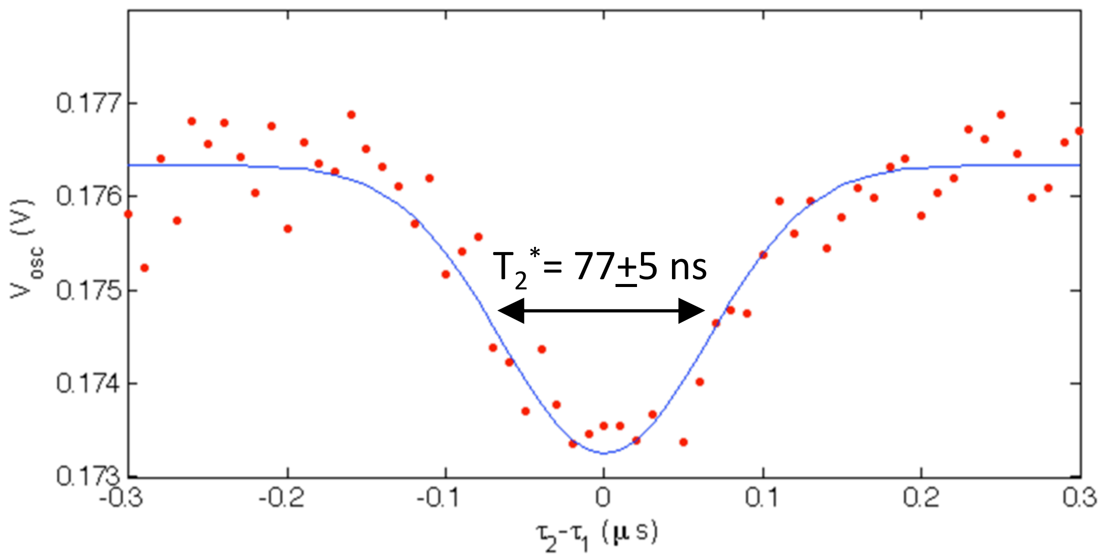

- T_2^* = 77 ns, consistent with ESR linewidth (FWHM) = 3.9 MHz
- Intrinsic control fidelity = 62%
- Similar to previous meas on nat. Si, T_2^* = 55 ns (J. J. Pla *et al.*, Nature (2012))

T_2 Measurement

D. R. Luhman

Hahn Echo with $\tau_1=\tau_2$:
Vary τ

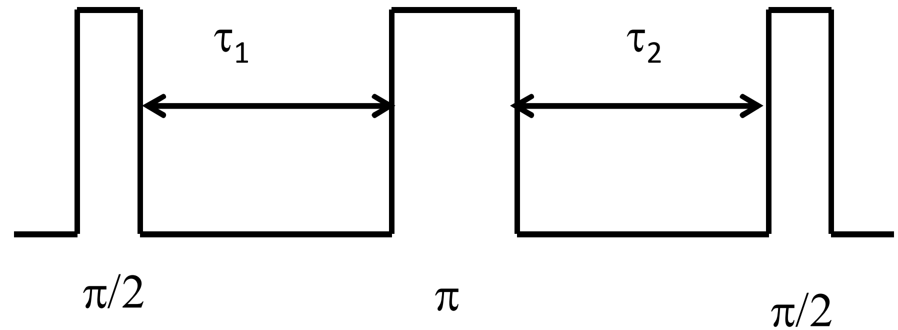

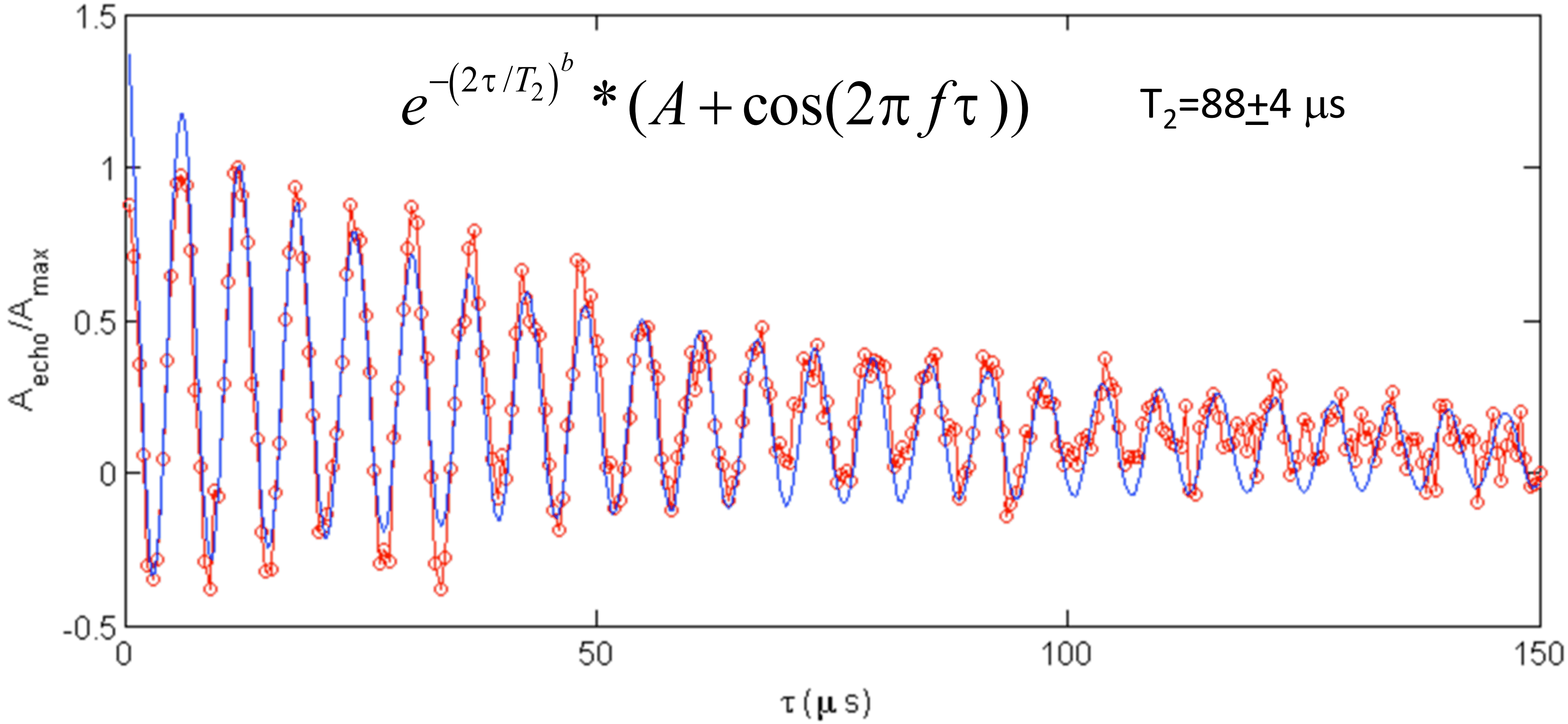

Unexpected Features

D. R. Luhman

ESR line shape

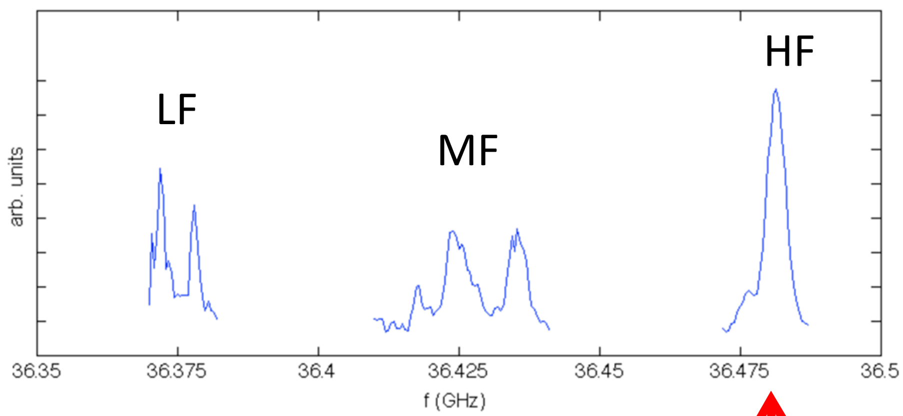

used for ESR

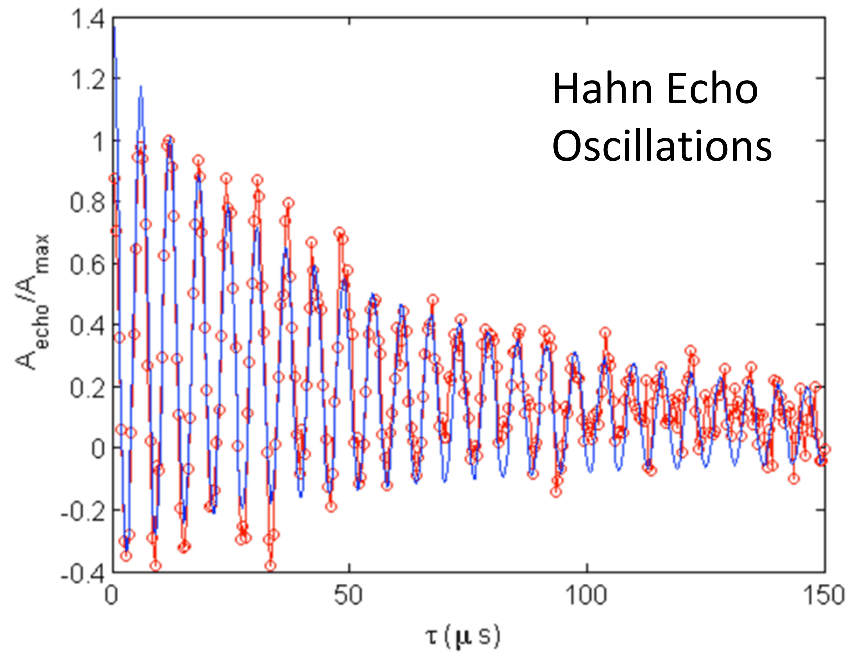

Possible explanation: P_2 Dimer

- Implant density high ($8x10^{11}/cm^2$)
- For J>>A, a center line is expected

Dimers in bulk P doped Si

Cullis and Marko, 1970
exchange effects in P doped Si

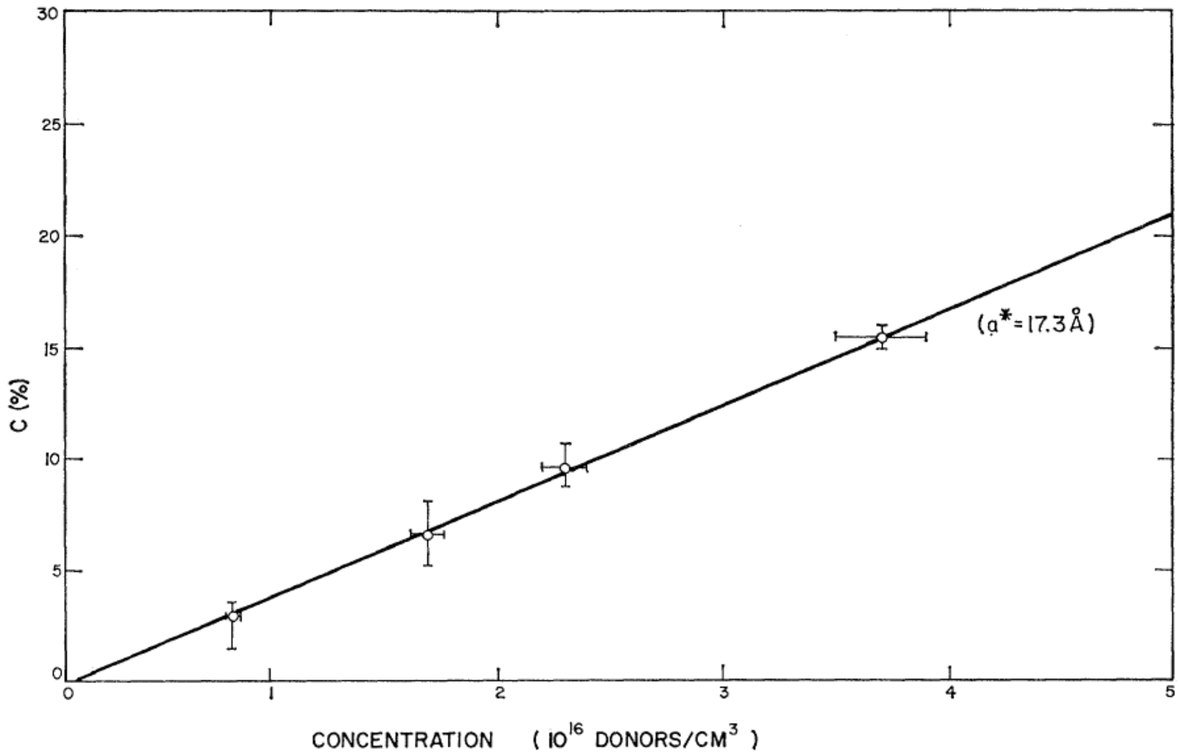

Ratio of the center line compared to outer lines for different P density. For the ESR device, the local implant density is ~1×10^{17} cm^{-3}

P2 Model for ESR data

D. R. Luhman, M. P. Lilly

$$H = \nu_e B + \nu_n B + J(S_1 \cdot S_2) + A_1(S_1 \cdot I_1) + A_2(S_2 \cdot I_2)$$

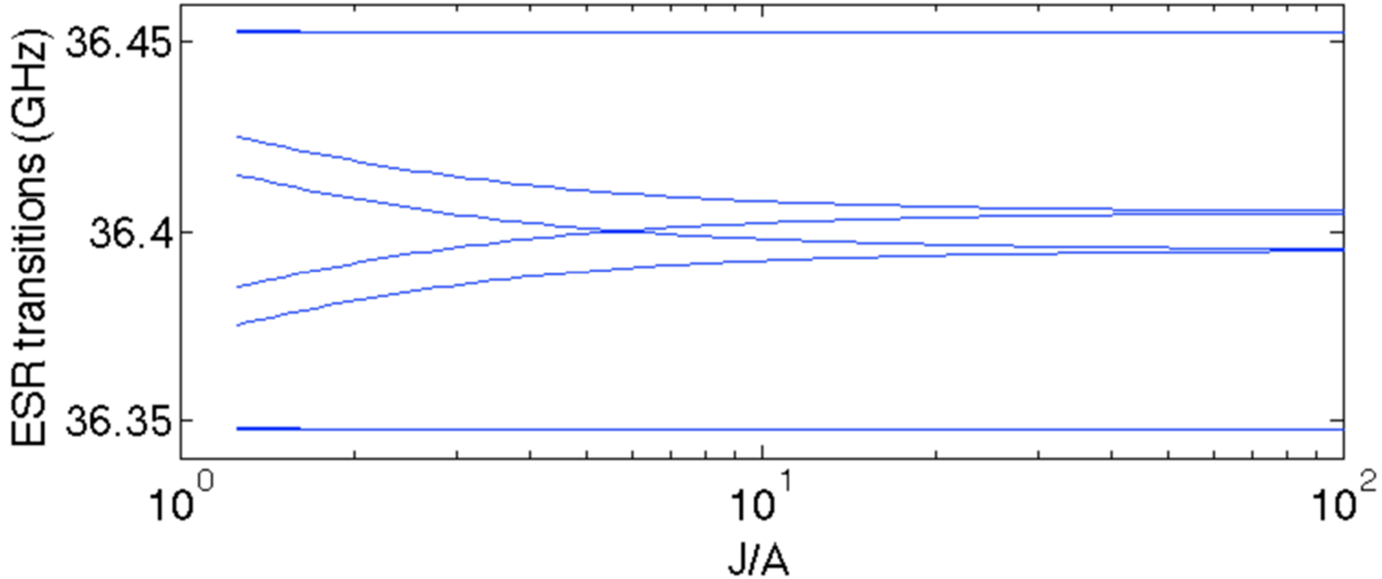

ΔA=14-24 MHz
J/A~2.5-4
Δf~165 kHz and independent of B

} Consistent with experiment

Enriched ^{28}Si: P donor ESR line

^{28}Si epilayer

- 2.5 μm thick
- 500 ppm ^{29}Si (ToF SIMS)

P Implant

- 45 keV implant
- range ~15 nm below SiO_2/Si interface
- Fluence: $4x10^{11}$ cm^{-2}

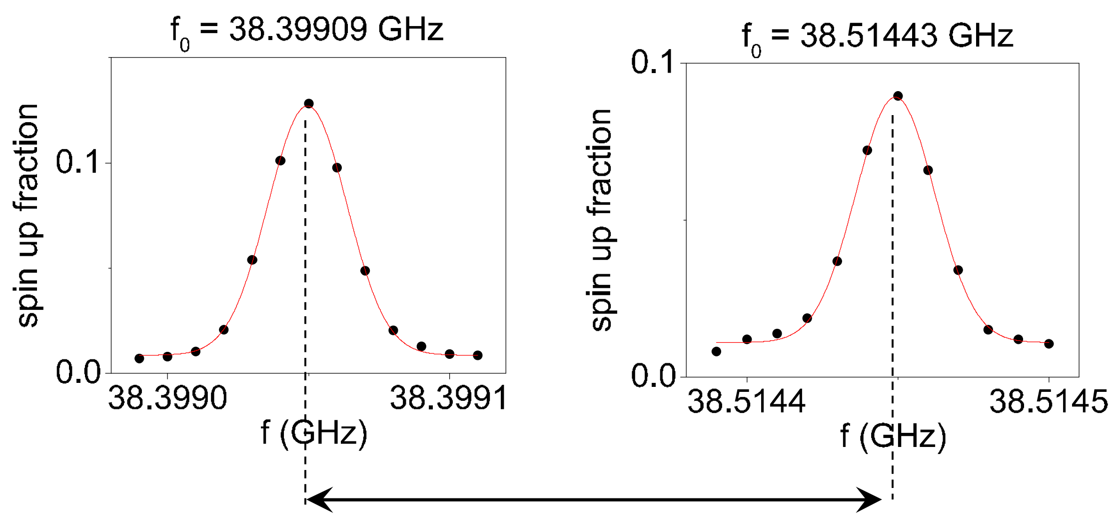

P hyperfine: Δf_0 = 115.3 MHz

low power linewidth

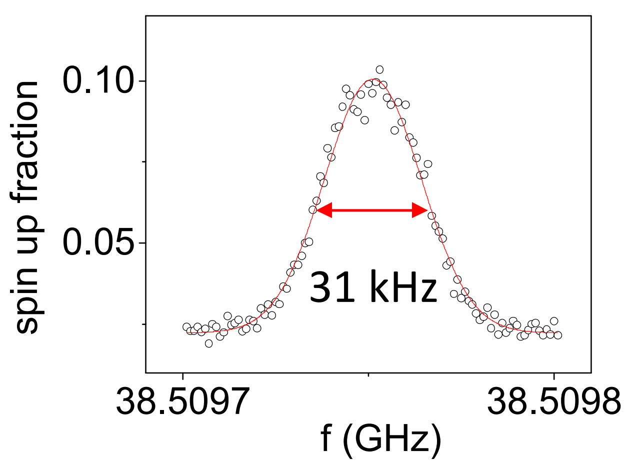

- Similar lines seen in two ^{28}Si ESR devices (115 – 116 MHz hyperfine w/ ~30 kHz linewidth)
- FWHM = 31 kHz → T_2^* = 10 us

Rabi oscillations

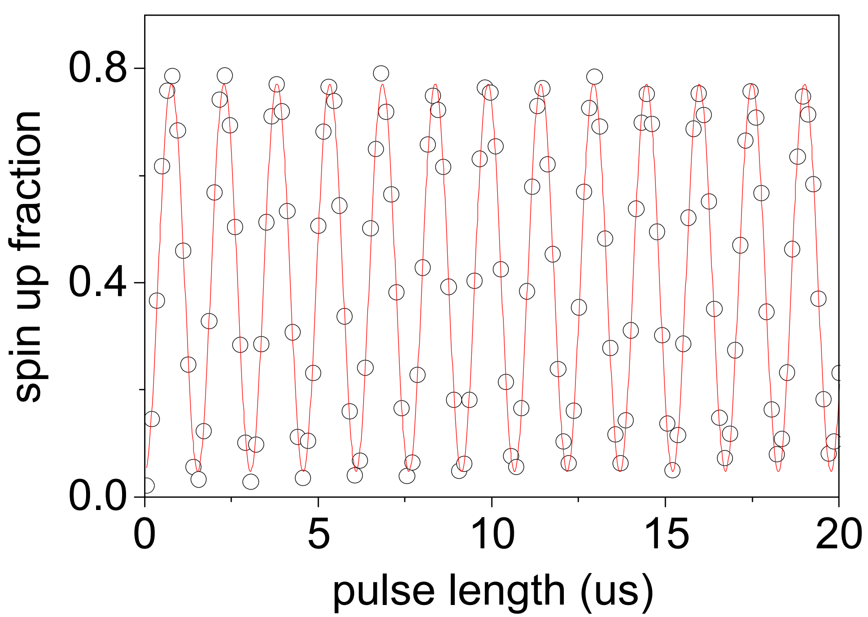

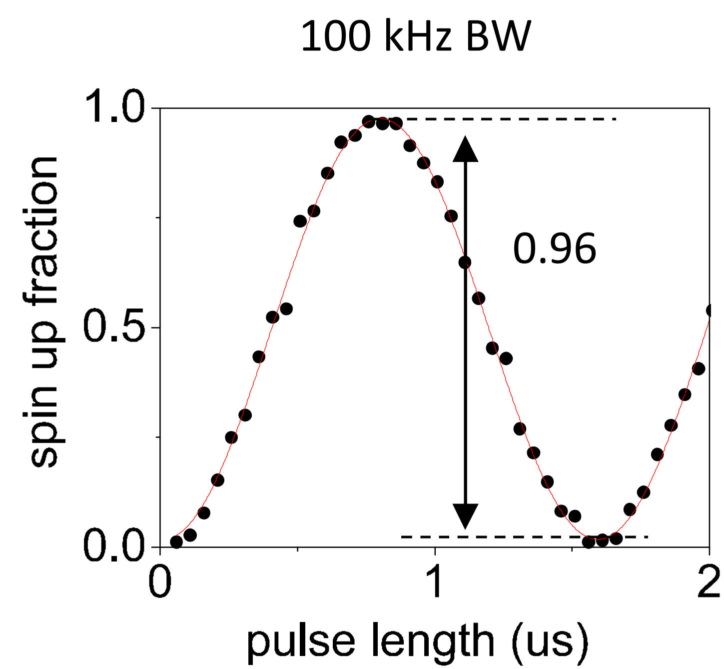

- Long lived Rabi oscillations
- Visibility reduced because readout BW was not optimized (~ 10 kHz)
  For example, fast spin-up tunneling events can be missed.
- Visibility ~ 96% (readout & initialization)

Ramsey fringes

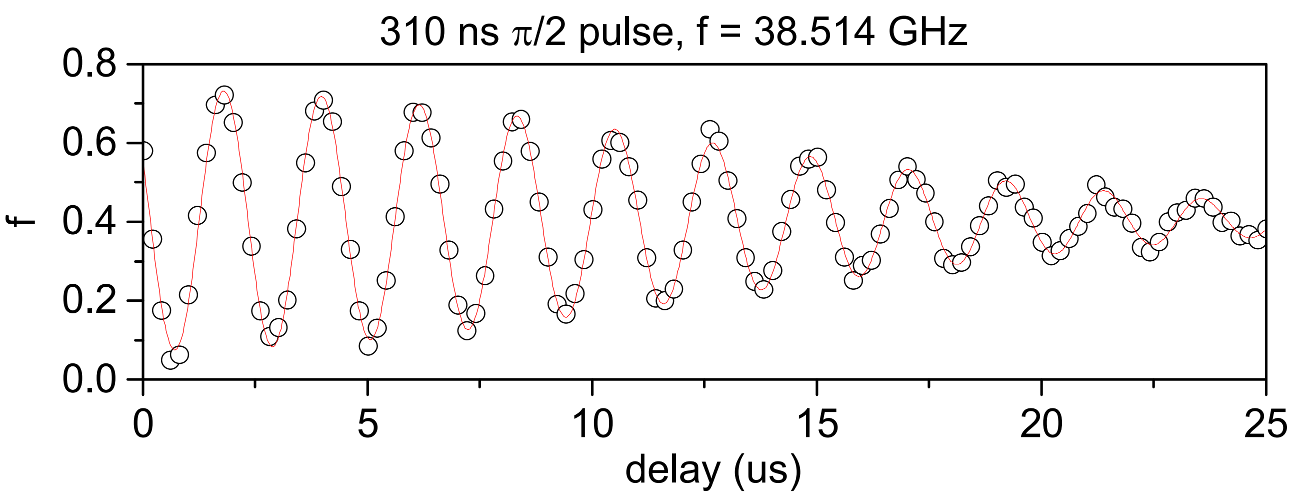

Fit envelope: $f = P_0 exp[-(t/T_2{}^*)^2] + P_\infty$

→ T_2* ~ 18 us

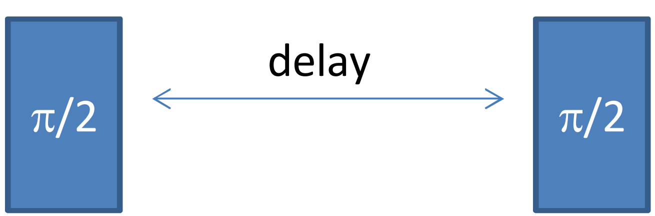

- ~ 0.5 MHz detuning from resonance
- T_2* value in same ballpark as linewidth estimate, but slightly longer (~18 us vs. 10 us)
- Intrinsic control fidelity ~ 99.99%

Hahn Echo

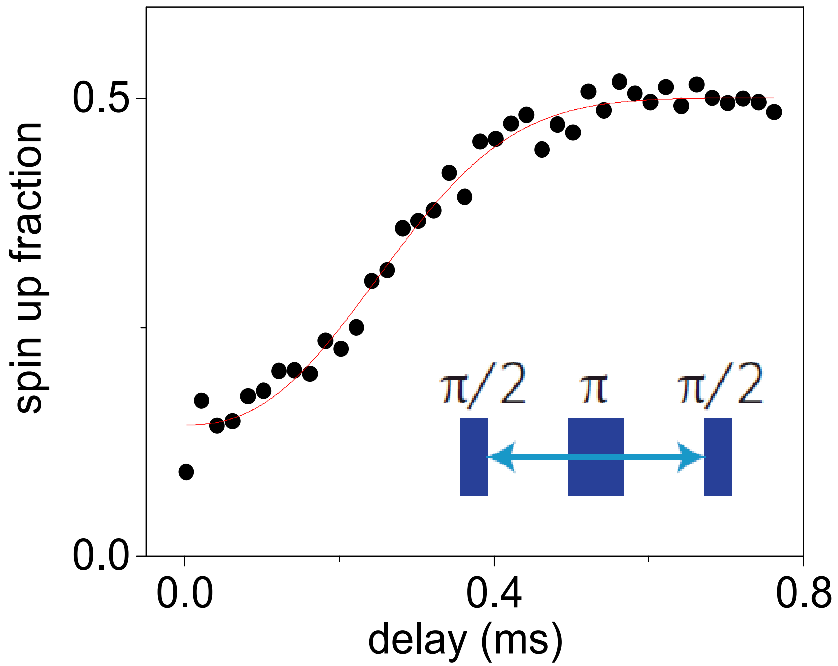

Fit: $f = P_0 exp[-(t/T_2)^n] + P_\infty$

→ T_2 = 0.31 ms, n = 2.4

- Echo T_2 in ballpark of previous meas of 0.95 ms, n = 3.5 (J. T. Muhonen et al., Nature Nano (2012))
- Exponent n = 2.4, for 1/f noise n = 2

Limiting factors for line width and T_2

- Observed ~30 kHz ESR line width in two samples
- T_2^* = 18 us shorter than meas T_2^* = 270 μs of J. T. Muhonen *et al*., Nat. Nano (2014) in 800 ppm ^{28}Si.
- Hahn echo T_2 = 0.3 ms vs. 0.95 ms from J. T. Muhonen *et al*.

Decoherence from nearby P donors?

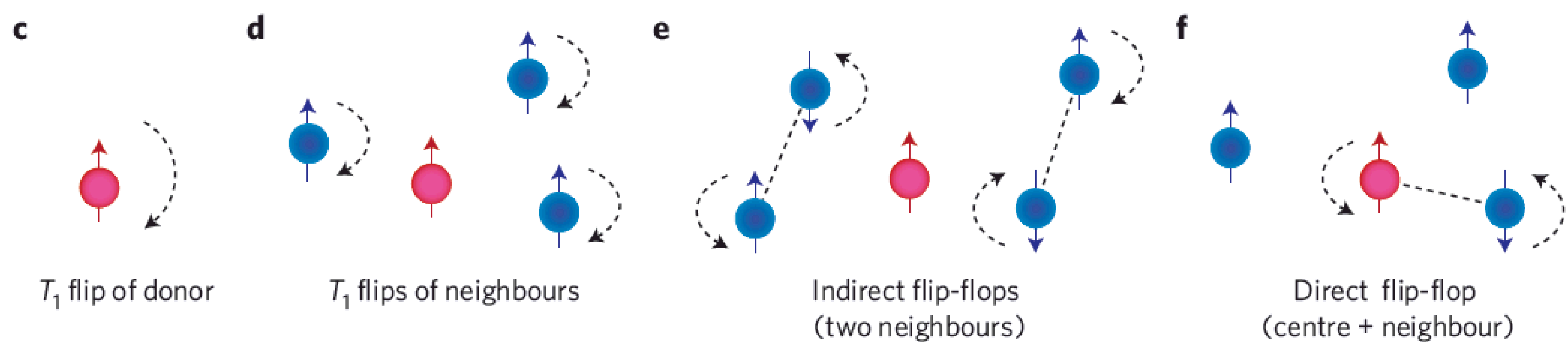

Tyryshkin *et al*., Nat. Mat. (2012)

W. Witzel

Calculated ESR line shapes

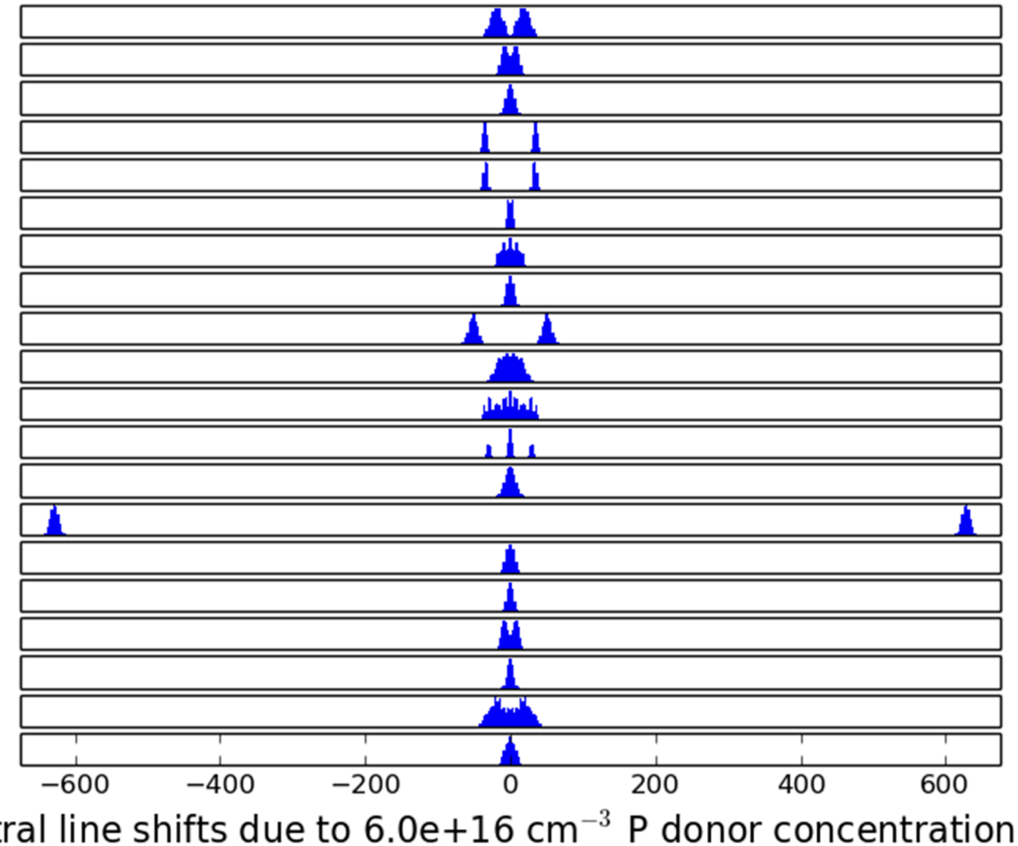

- Each row: different possible spectra for a given constellation of neighboring spins
- Dynamics?

Sandia National Laboratories

Dilution refrigerator acoustic noise (pulse tube)

Voltage from pickup coil at sample position

FFT

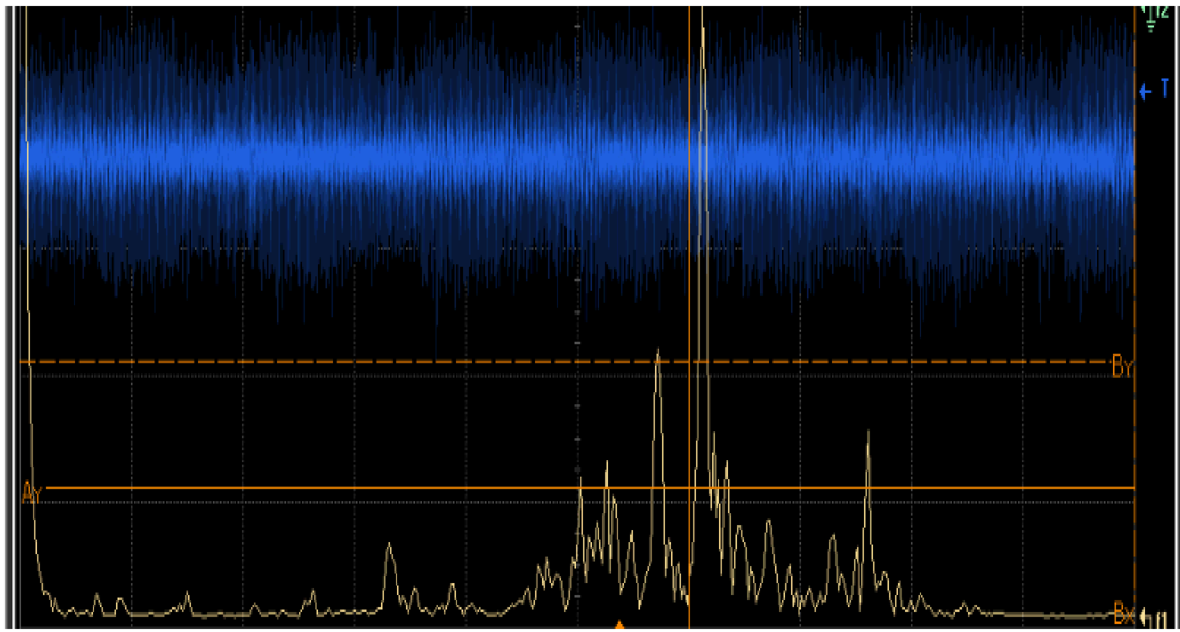

0 1 2

f (kHz)

Rough estimate: ~ 10 um of vibration, ~100 kHz linewidth

Sandia National Laboratories

R. Blume-Kohout, E. Nielsen

Gate Set Tomography

Operator	Hilbert-Schmidt vector (Pauli basis)	Matrix
ρ_0	0.7206 −0.0168 −0.0185 0.6741	$\begin{pmatrix} 0.9862 & 0.0177e^{i2.3} \\ 0.0177e^{-i2.3} & 0.0328 \end{pmatrix}$
E_0	0.6929 0.0328 −0.0029 −0.6516	$\begin{pmatrix} 0.0292 & 0.0233e^{i0.1} \\ 0.0233e^{-i0.1} & 0.9507 \end{pmatrix}$

Table 5: **The GST estimate of the SPAM operations.** Compare to Table 1.

Gate	Superoperator (Pauli basis)
Gi	$\begin{pmatrix} 0.9992 & -0.0007 & 0.006 & 0.004 \\ -0.002 & 0.953 & 0.0227 & 0.0008 \\ 0.0114 & -0.0115 & 0.9361 & 0.0065 \\ 0.0027 & -0.0009 & -0.0061 & 1.0047 \end{pmatrix}$
Gx	$\begin{pmatrix} 1.0003 & 0.0087 & -0.0354 & -0.0027 \\ -0.0048 & 0.9352 & 0.1054 & 0.0869 \\ 0.0089 & 0.1197 & -0.0091 & -0.9284 \\ 0.0051 & -0.1363 & 0.9467 & -0.0346 \end{pmatrix}$
Gy	$\begin{pmatrix} 0.999 & 0.0496 & -0.008 & -0.0219 \\ 0.0014 & -0.0115 & 0.099 & 0.9425 \\ -0.0072 & 0.1273 & 0.929 & -0.1308 \\ 0.0145 & -0.9091 & 0.0914 & -0.0356 \end{pmatrix}$

Table 6: **The GST estimate of the logic gate operations.** Compare to Table 2.

- Gate set tomography (GST) was used to characterize qubit. Maximum length base sequence L = 8.
- State preparation and measurement error (SPAM) is ~6%
- Idle gate error is ~2.5%.
- X and Y rotation errors ~5%. Looks like phase error between X and Y. Possibly instrumental error which can be improved.

Sandia National Laboratories

Conclusions

Natural Silicon:

- Three ESR lines (dimer)
- Coherence
  - $T_2^* = 77$ ns
  - $T_2 = 88$ μs (Hahn Echo)

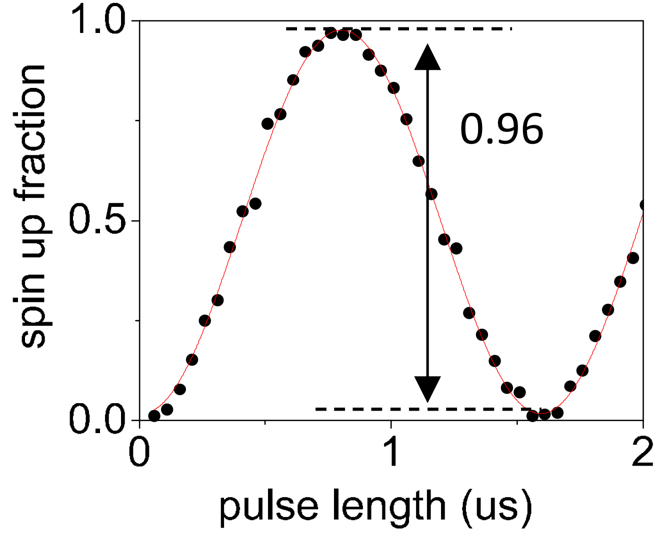

Enriched ^{28}Si (500 ppm):

- Two ESR lines
- Control Fidelity 95% (GST)
- Rabi Visibility 96%
- Coherence
  - $T_2^* = 18$ μs
  - $T_2 = 0.3$ ms (Hahn Echo)

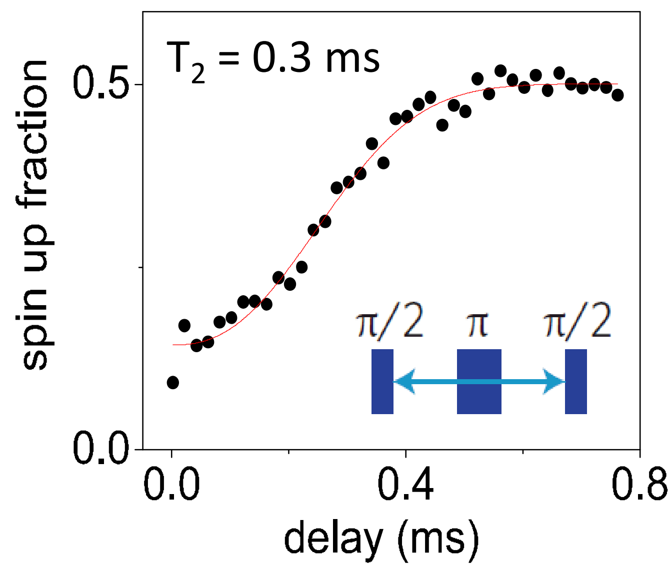

Acknowledgements

- QIST contributors at SNL
  Qubit fab: M. Busse, J. Dominguez, T. Pluym, B. Silva, G. Ten Eyck, J. Wendt, S. Wolfley
  Qubit Measurement: N. Bishop, S. Carr, S. Eley, M. Lilly, T.-M. Lu, D. Luhman, K. Nguyen, M. Rudolph, M. Singh, L. Tracy, M. Wanke
  Advanced fabrication (two qubit): E. Bielejec, E. Bussmann, A. MacDonald, B. McWatters, S. Misra, D. Perry, D. Serkland, G. Subramanian, E. Yitamben
  Device modeling: J. Gamble, T. Jacobson, R. Muller, E. Nielsen, I. Waldmueller, W. Witzel, R. Young

- Joint research efforts with external community:
  – Australian Centre for Quantum Computing and Communication Technology (A. Dzurak, L. Hollenberg, D. Jamieson, A. Morello, S. Rogge, M. Simmons)
  – Princeton University (S. Lyon)
  – NIST (N. Zimmerman)
  – U. Maryland (S. Das Sarma)
  – National Research Council (A. Sachrajda)
  – U. Sherbrooke (P. Harvey-Collard & M. Pioro-Ladriere)
  – Purdue University (G. Klimeck & R. Rahman)
  – U. New Mexico (A. Shirkhorshidian & P. Zarkesh-Ha)
  – U. Wisconsin (M. Eriksson, M. Friesen)

Auxiliary slides

Lower power NMR sweep

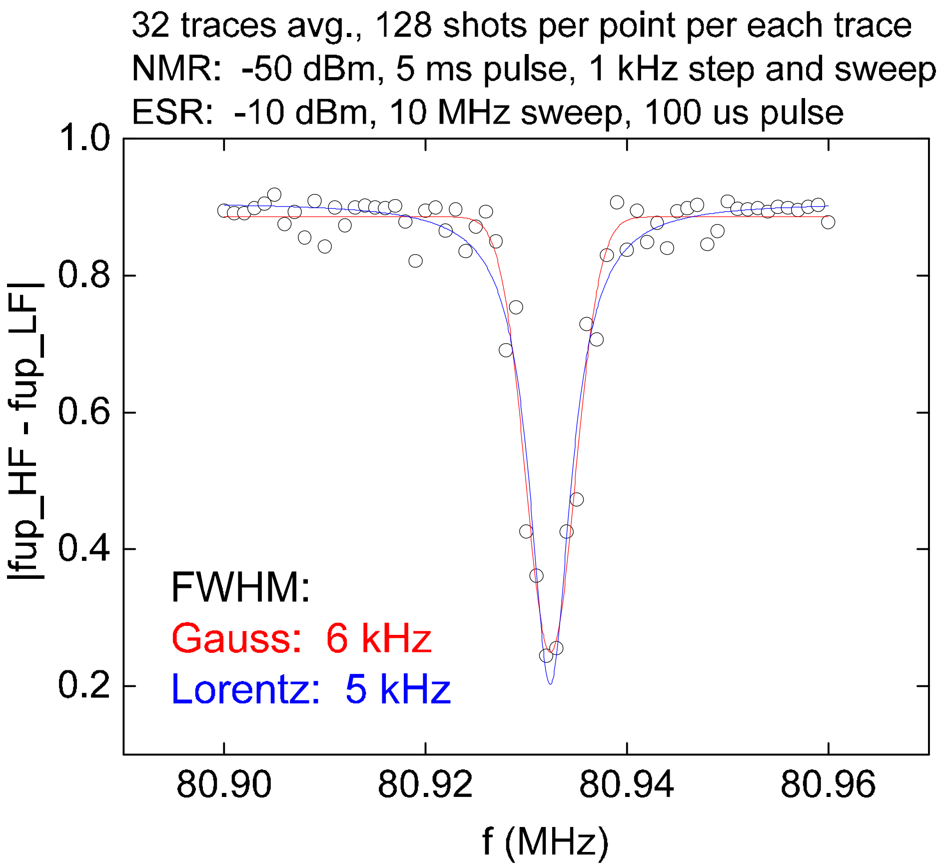

High power ESR sweeps

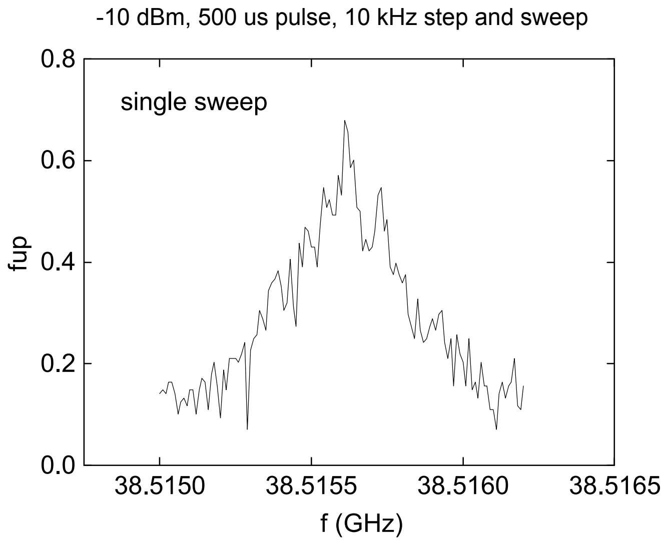

repeats of single sweep

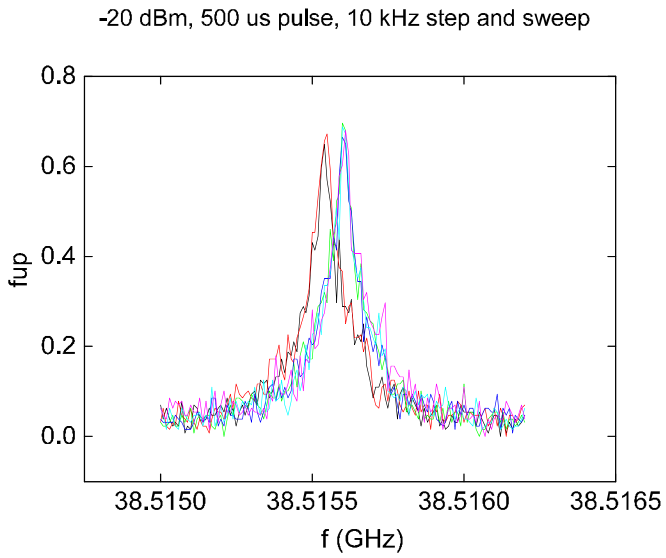

~10 min per trace

jump ~ 60 kHz
similar to jump in slide 12

Ramsey beat frequency was ~ 200 kHz

Nuclear Rabi Osc. (electron down spin loaded on donor)

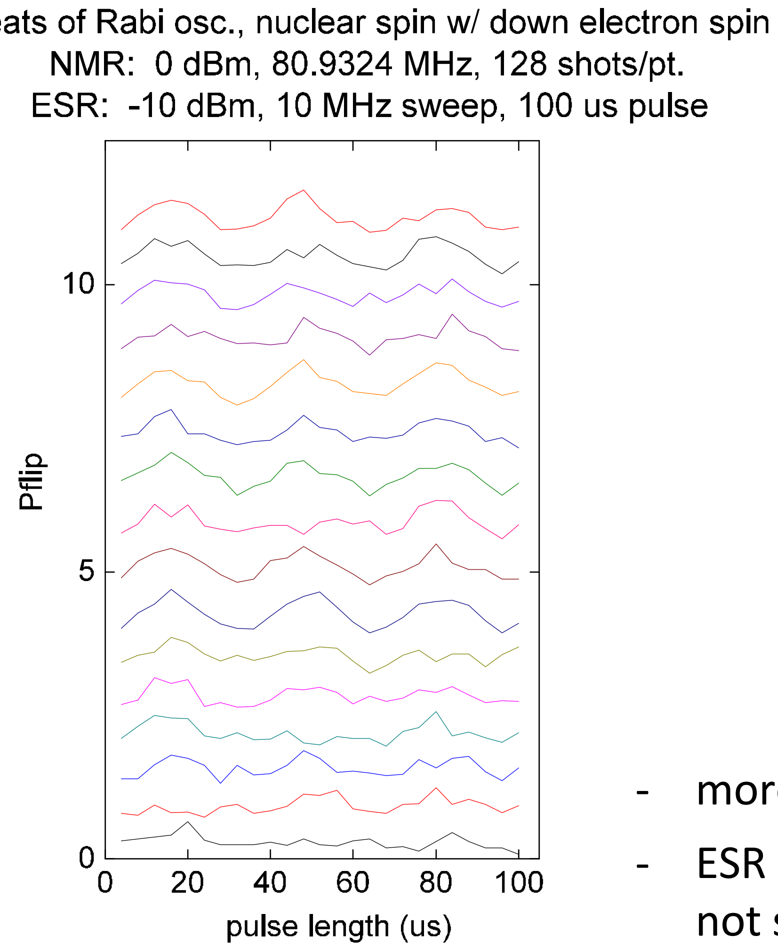

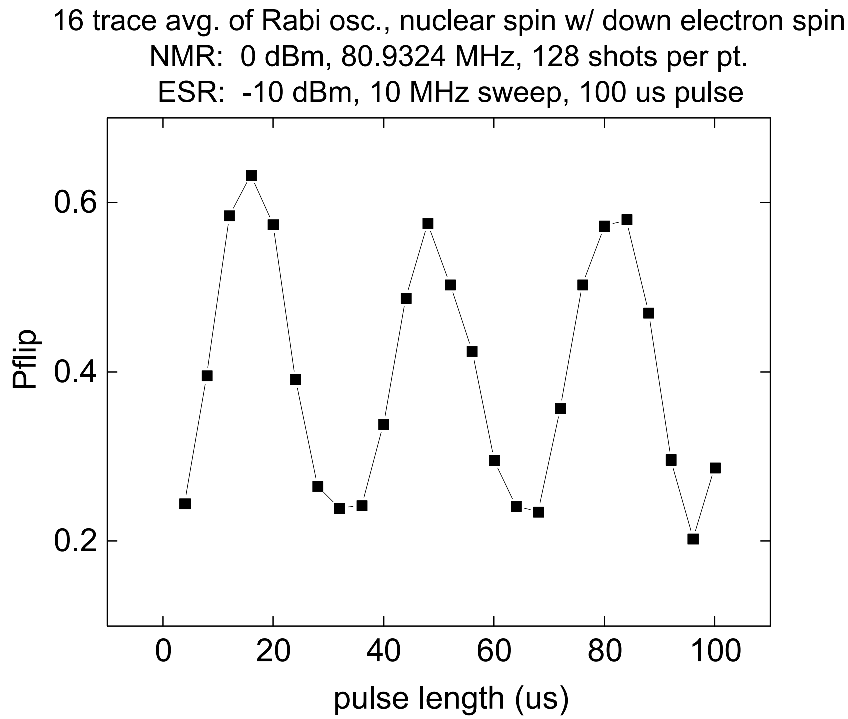

- more power reaching sample than I expected
- ESR adiabatic flip and readout should be ~ 0 to 0.9, not sure why Pflip contrast for nuclear flip is low (oscillations noisy)
- Info about charge noise?

High power ESR sweep to flip neighboring P electron spins

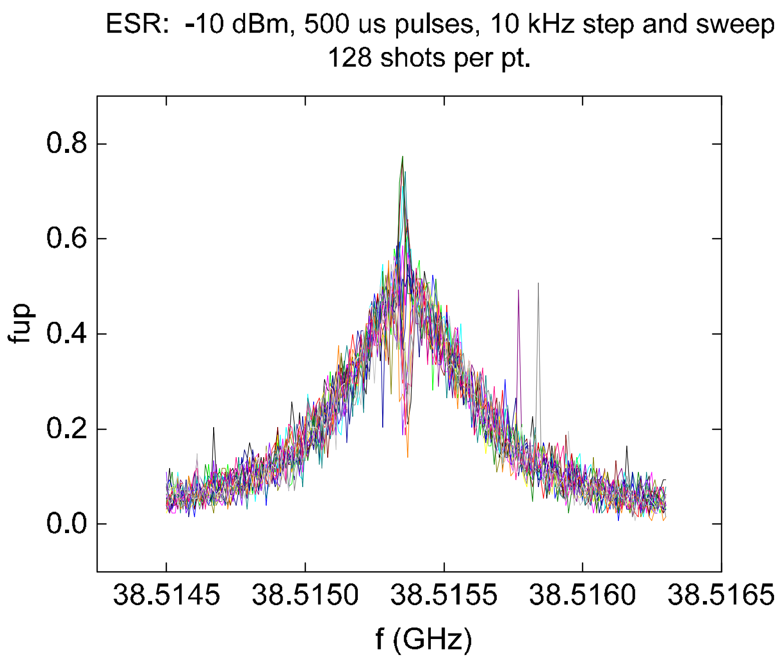

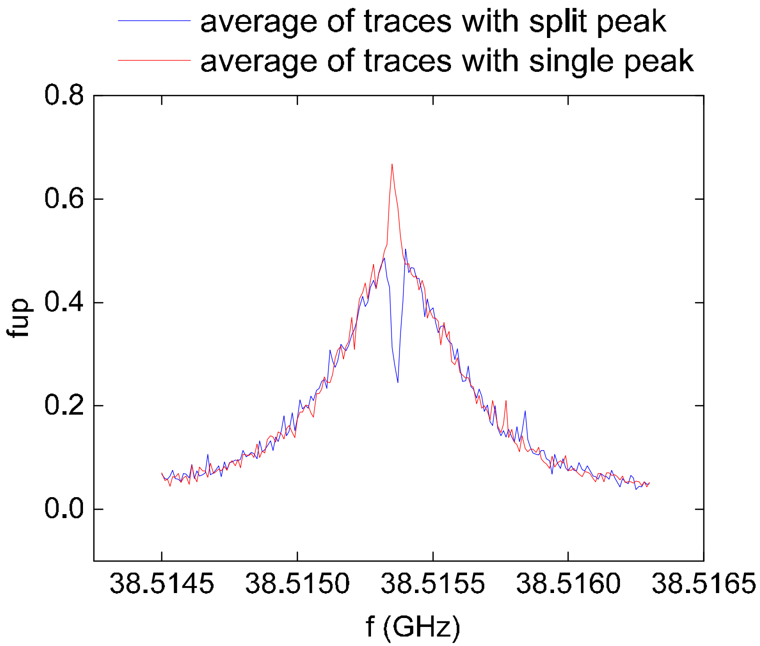

Could this be this neighbor P nuclear spin up vs. down?

ESR sweep with P NMR pulse

No NMR

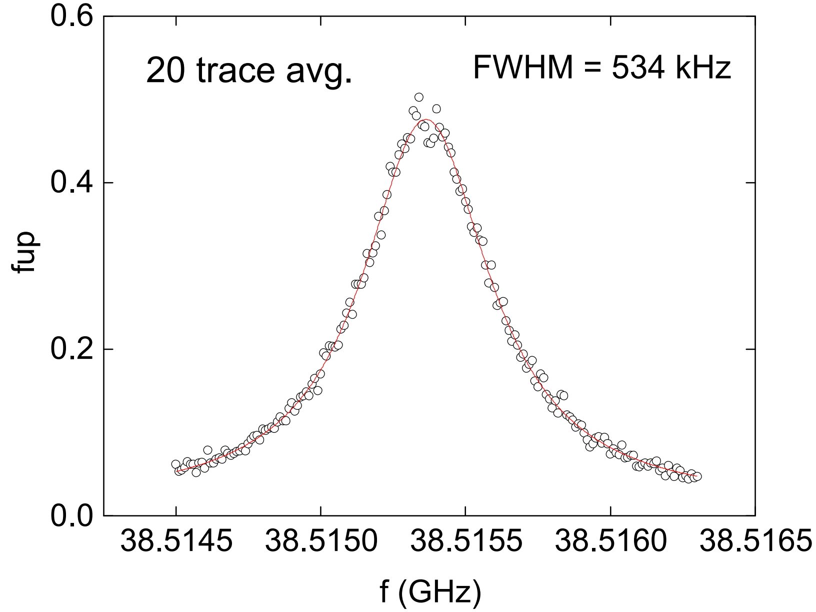

P NMR & ESR sweep
ESR: -10 dBm, 20 kHz step and sweep, 500 us pulse
NMR: -3 dBm, 5 ms pulse, 79 to 83 MHz

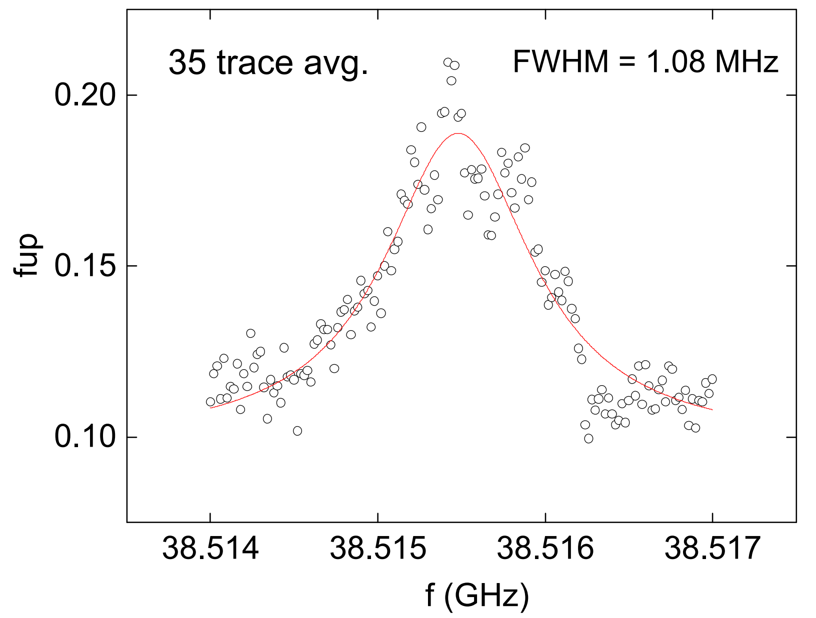

ESR peak width increase with 4 MHz P nuclear sweep?

W. Witzel

Hyperfine shifts from ^{29}Si?

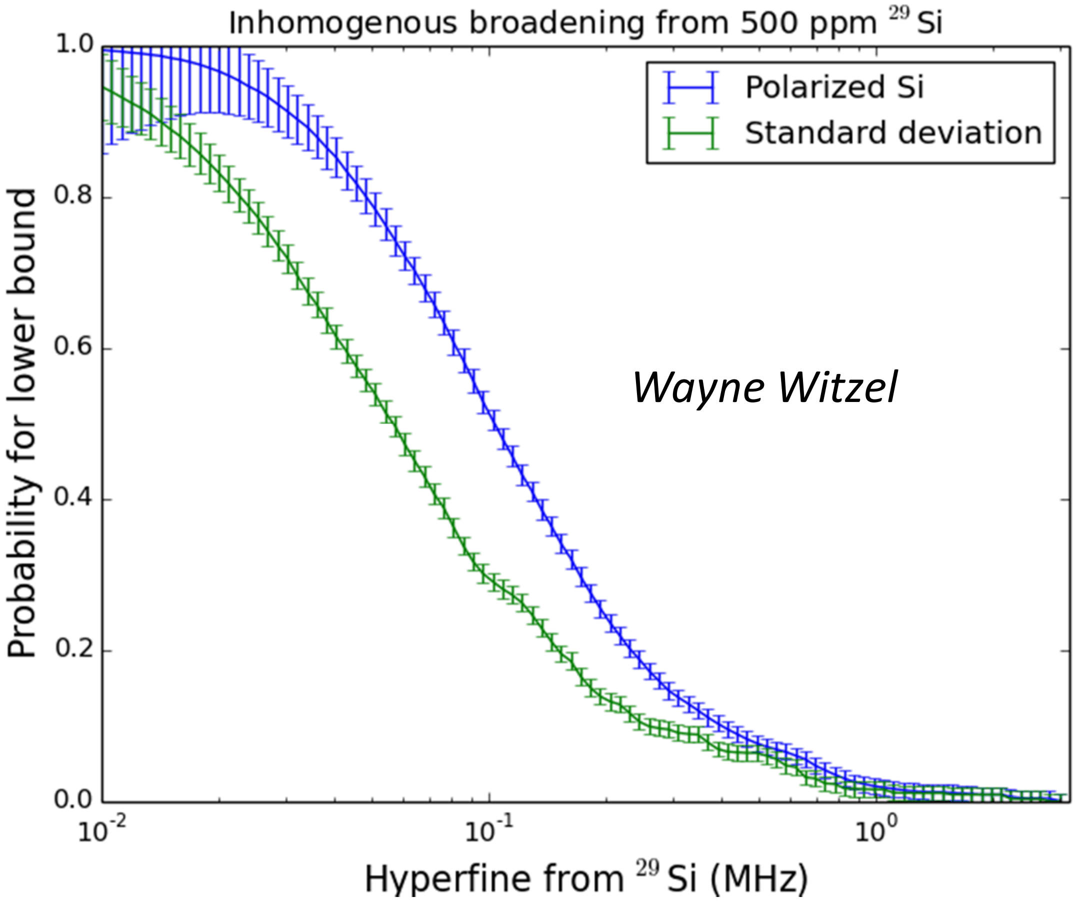

- Every sample will have different ^{29}Si constellation.
- 30 kHz linewidth seems reasonable, but it is suspicious that is occurred in two samples.
- Dynamics? How are background spins changing during measurement?

Calculated ESR line shapes

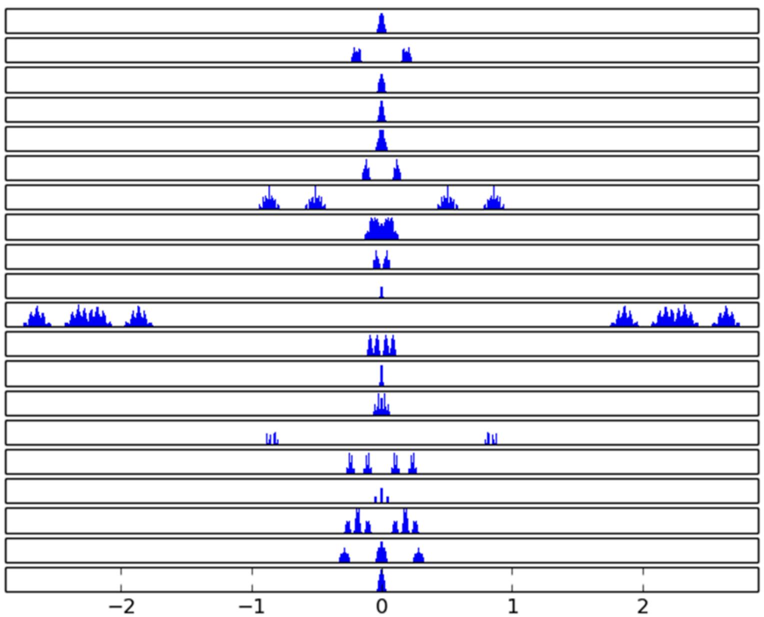

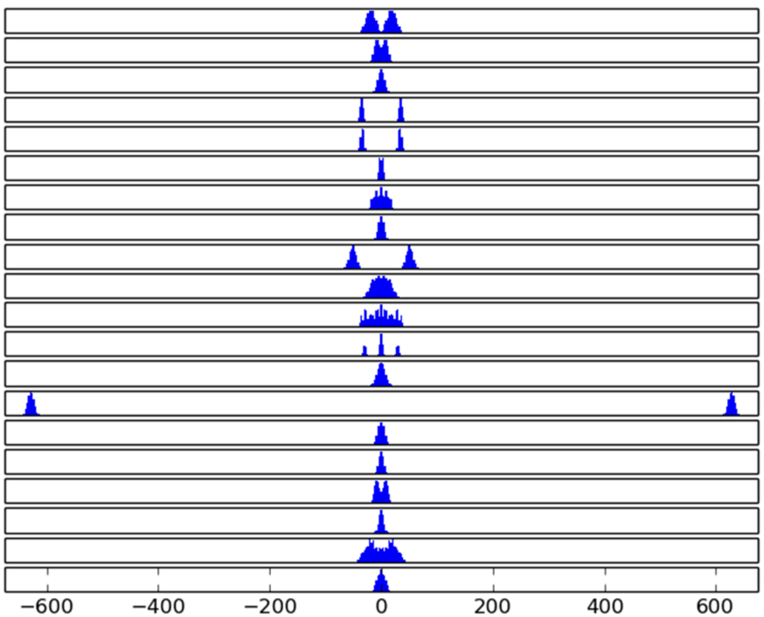

- Each row: different possible spectra for a given constellation of neighboring spins
- From experiment: P density $6x10^{16}/cm^3$, 500 ppm ^{29}Si

Beating in Rabi oscillations

Each trace identical repeat

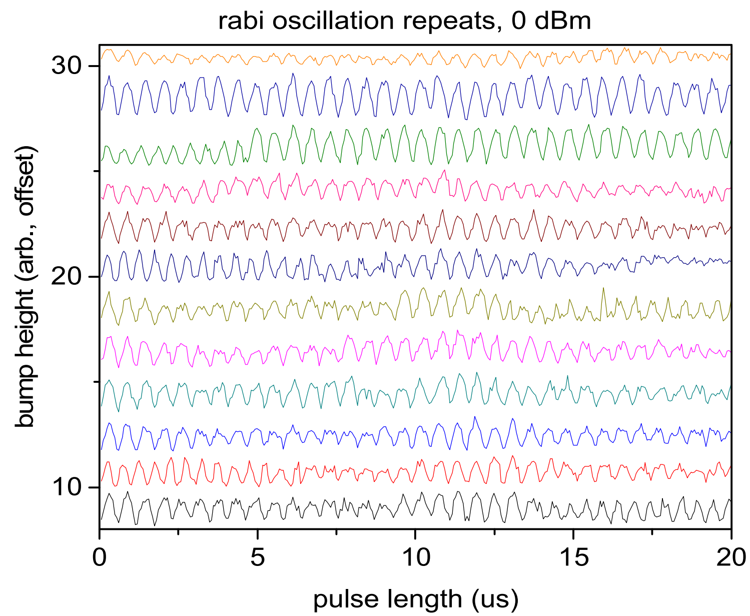

0 dBm
128 averages

Ramsey Fringes

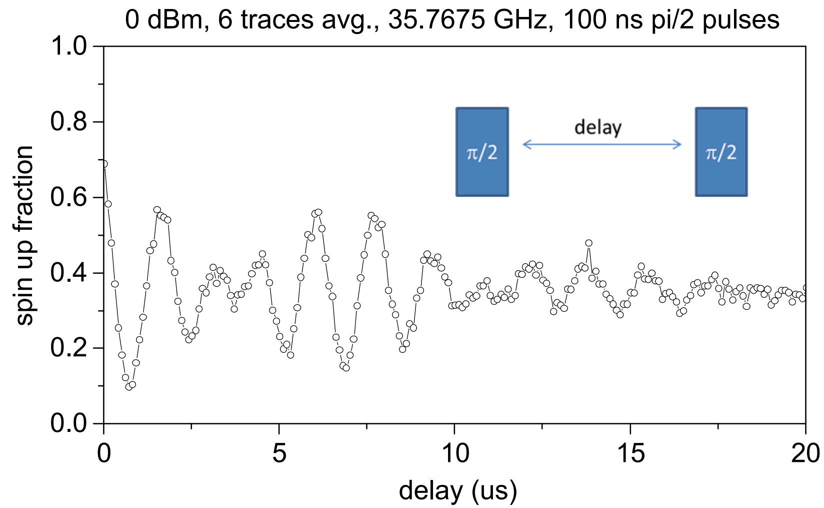

Beat frequency ~ 200 kHz

Complex line structure

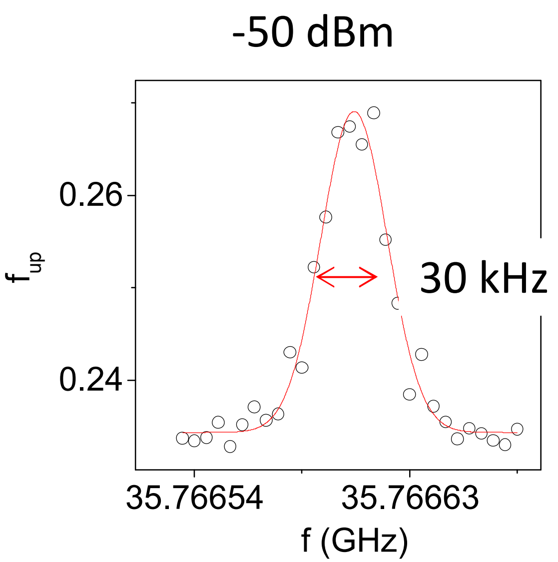

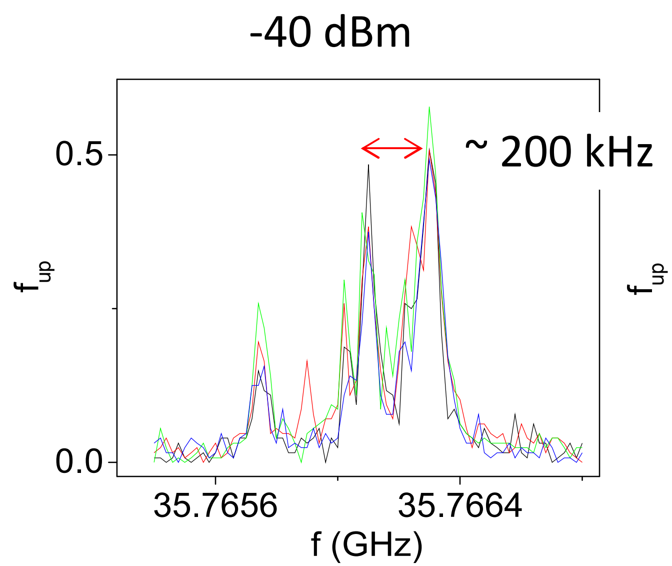

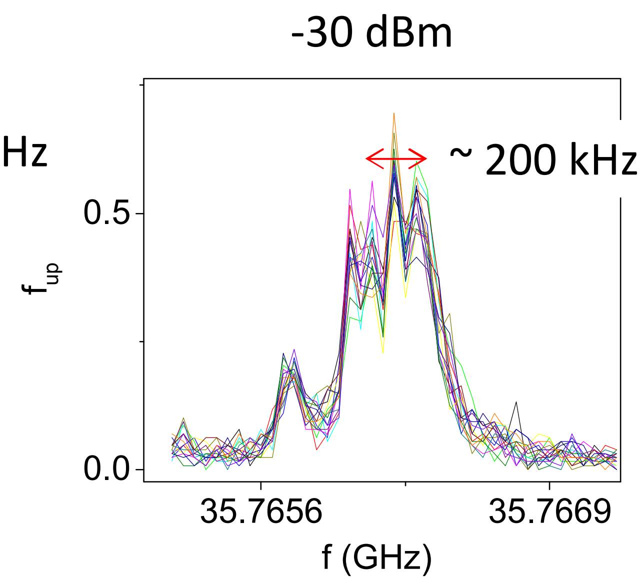

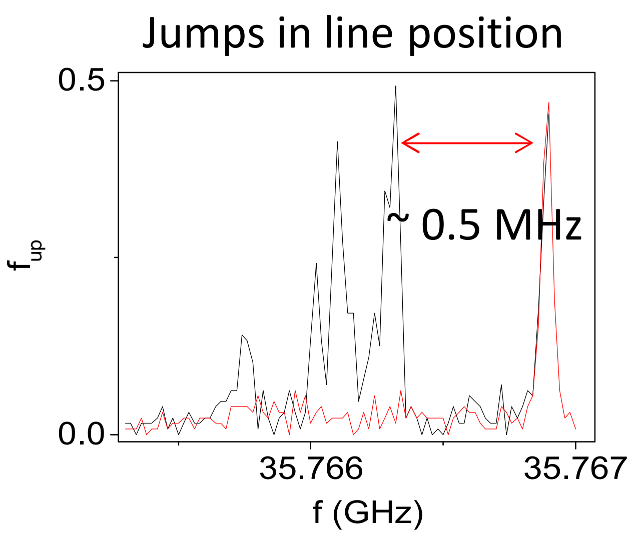

- Additional transitions apparent at higher microwave power
- Discrete jumps in position of line over hour long time scales

Sandia National Laboratories

ESR Spectrum

D. R. Luhman

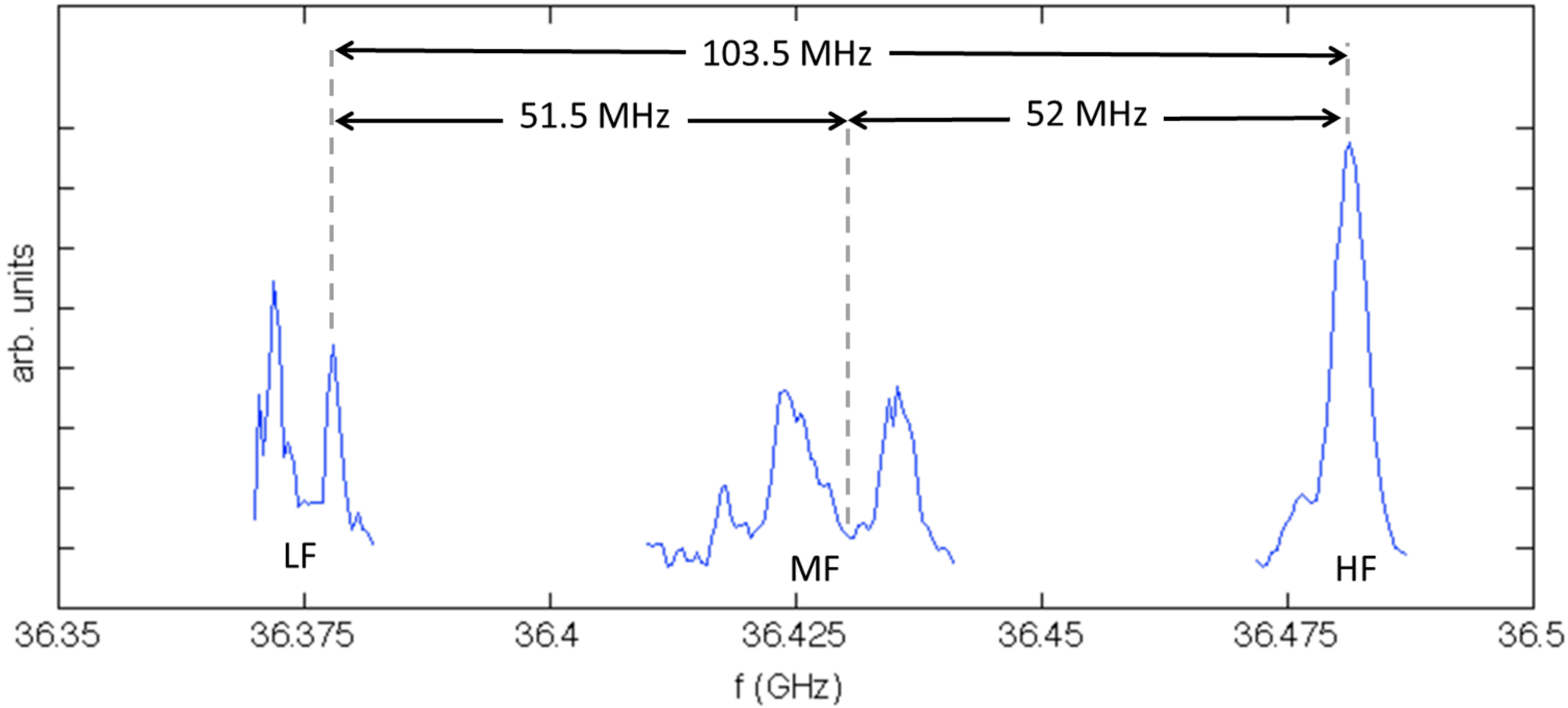

HF Splitting: 5.26 $\pm$ 0.09 MHz
LF Splitting: 6.0 $\pm$ 0.2 MHz

Likely due to nearby ^{29}Si

HF line used for Rabi Oscillation, T_2, T_2^*

Sandia National Laboratories

Hahn Echo Oscillations

D. R. Luhman

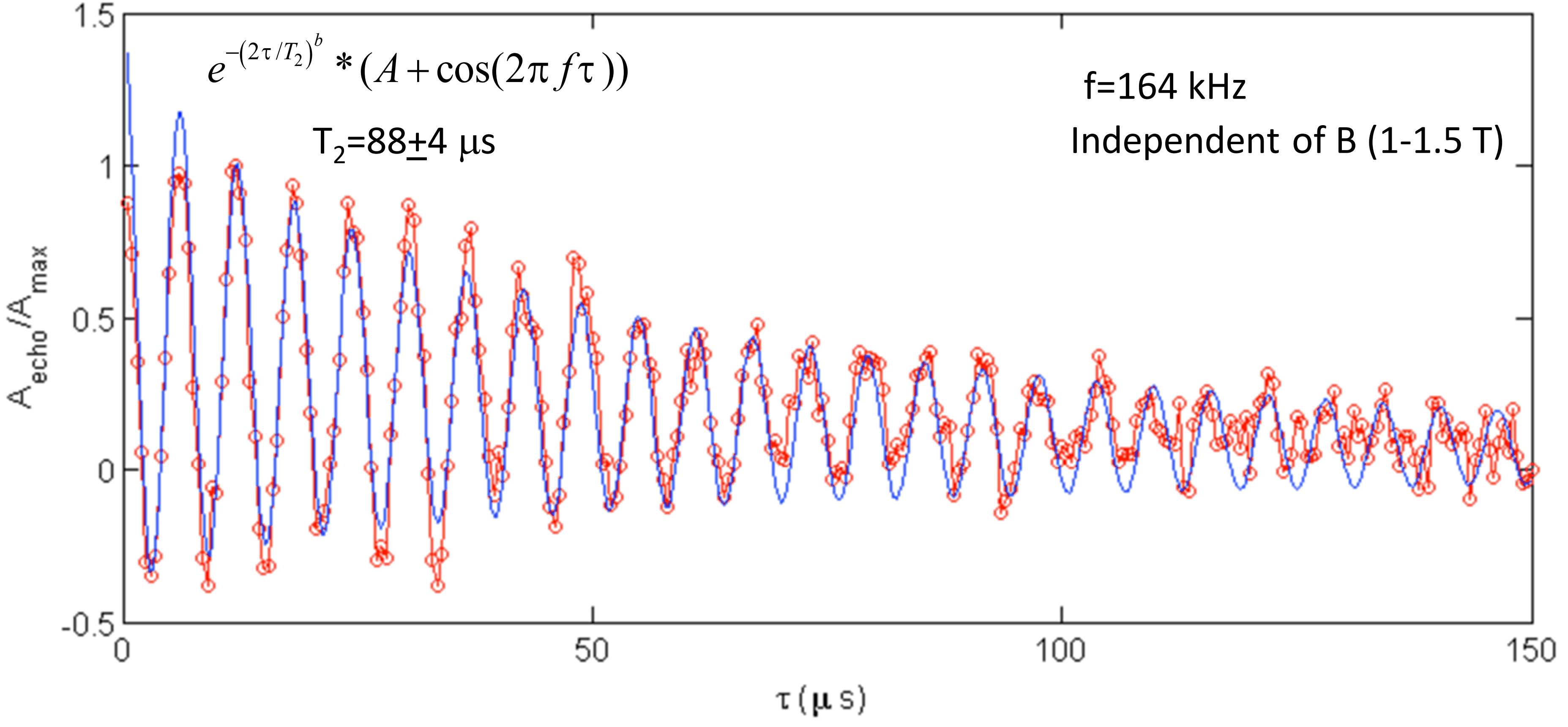

Sandia National Laboratories

Phosphorus dimer exchange model

W. Witzel

H = ν_eB + ν_nB + J(S1*S2) + A1(S1*I1) + A2(S2*I2)

spin basis: ($m_{s,1}$, $m_{s,2}$, $m_{I,1}$, $m_{I,2}$)

$$|\uparrow\uparrow\Uparrow\Uparrow\rangle \; |\uparrow\uparrow\Uparrow\Uparrow\rangle \; |\uparrow\uparrow\Uparrow\Uparrow\rangle \; |\uparrow\uparrow\Uparrow\Uparrow\rangle \; |\uparrow\uparrow\Uparrow\Uparrow\rangle \; |\uparrow\uparrow\Uparrow\Uparrow\rangle \; |\uparrow\uparrow\Uparrow\Uparrow\rangle \; |\uparrow\uparrow\Uparrow\Uparrow\rangle \; |\uparrow\uparrow\Uparrow\Uparrow\rangle \; |\uparrow\uparrow\Uparrow\Uparrow\rangle \; |\uparrow\uparrow\Uparrow\Uparrow\rangle \; |\uparrow\uparrow\Uparrow\Uparrow\rangle \; |\uparrow\uparrow\Uparrow\Uparrow\rangle \; |\uparrow\uparrow\Uparrow\Uparrow\rangle \; |\uparrow\uparrow\Uparrow\Uparrow\rangle \; |\uparrow\uparrow\Uparrow\Uparrow\rangle$$

$$\frac{1}{4}\left(\begin{array}{cccccccccccccccc}
4\nu+J+A+a & & & & & & & & & & & & & & & \\
 & 4\nu+A-a+J & & & * & & & & & & & & & & & \\
 & & 4\nu-A+a+J & & & & & & * & & & & & & & \\
 & & & 4\nu-A-a & & & * & & & * & & & & & & \\
 & * & & & A-a-J & & & & * & & & * & & & & \\
 & & & & & A+a-J & & & & * & & & * & & & \\
 & & & * & & & -A-a-J & & & & * & & & & & \\
 & & & & & & & -A+a-J & & & & * & & & & \\
 & & * & & * & & & & -A+a-J & & & & & & & \\
 & & & * & & * & & & & -A-a-J & & & * & & & \\
 & & & & & & * & & & & A+a-J & & & & & \\
 & & & & & & & * & & & & A-a-J & & & * & \\
 & & & & & & * & & & & & & -4\nu-A-a+J & & & \\
 & & & & & & & * & & & & & & -4\nu-A+a+J & & \\
 & & & & & & & & & & & * & & & -4\nu+A & \\
 & & & & & & & & & & & & & & & -\nu
\end{array}\right)$$

P2 ESR Spectrum

D. R. Luhman, M. P. Lilly

$(A_1+A_2)/2=105$ MHz
$A_1=115$ MHz $A_2=95$ MHz

8 most probable ESR transitions

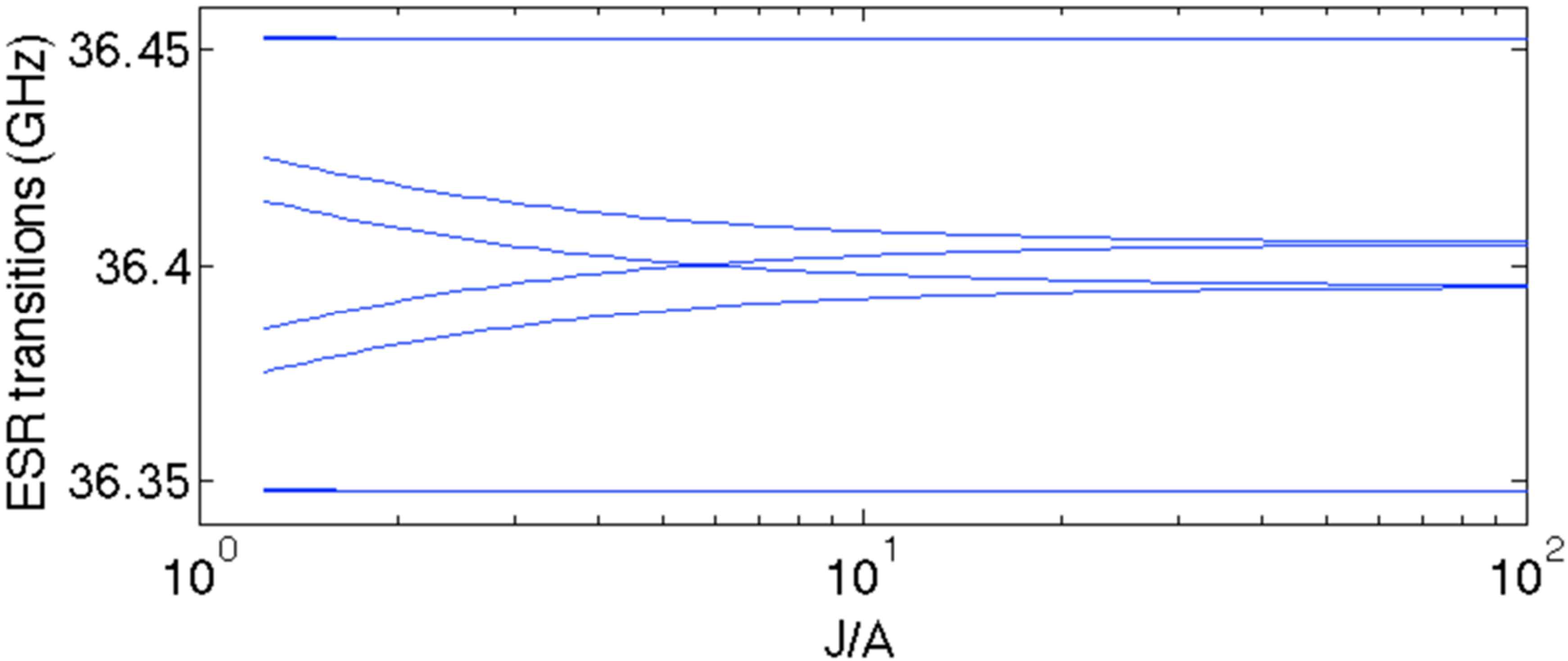

Kalra et al. PRX **4** (2014)
Shankar, Tyryshkin, Lyon arxiv.1409.3534

A dimer with J>A can produce central lines

P2 ESR Spectrum

D. R. Luhman, M. P. Lilly

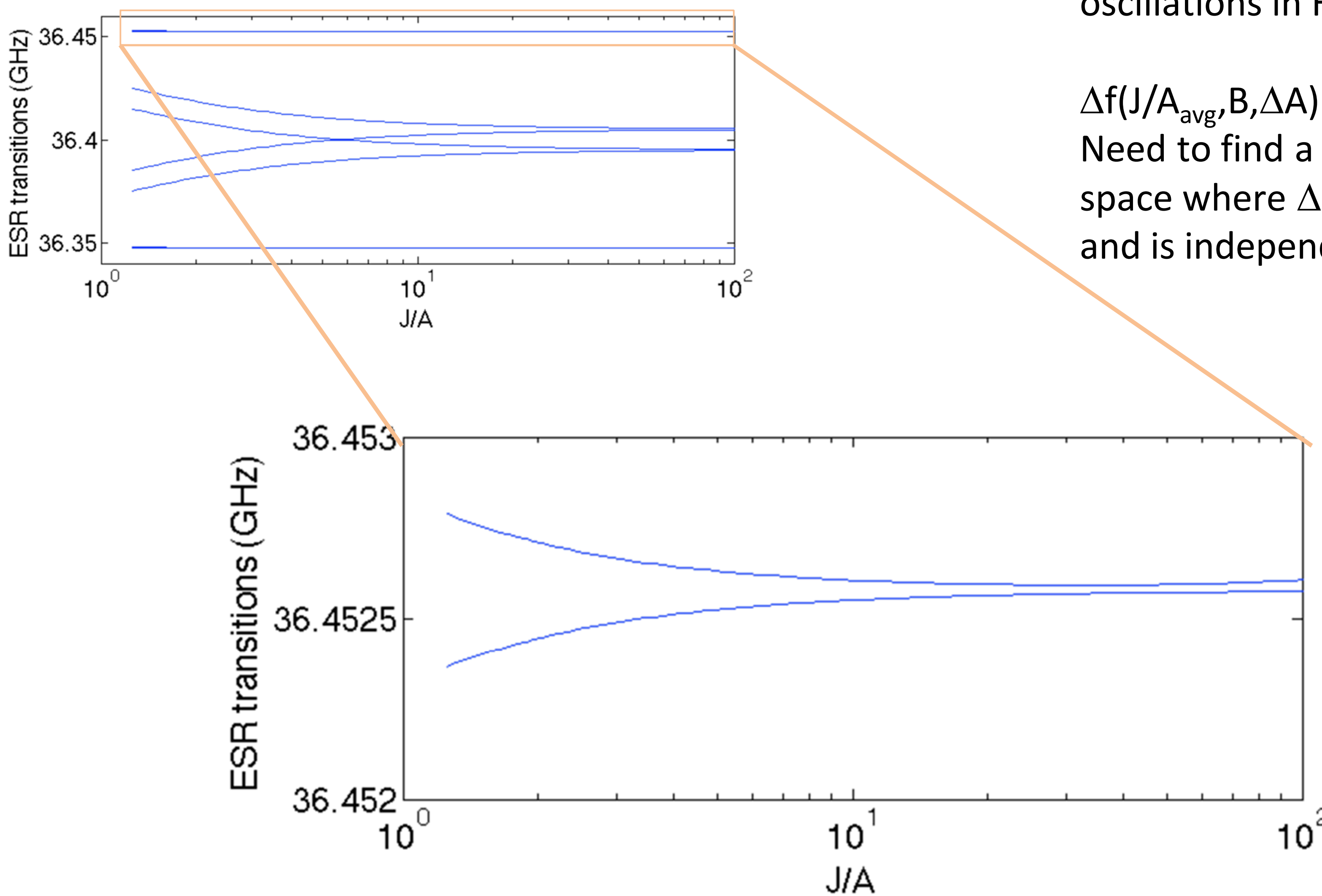

Difference, Δf, may lead to oscillations in Hahn Echo

$\Delta f(J/A_{avg}, B, \Delta A)$

Need to find a parameter space where Δf=164 kHz and is independent of B

Center Line

D. R. Luhman, M. P. Lilly

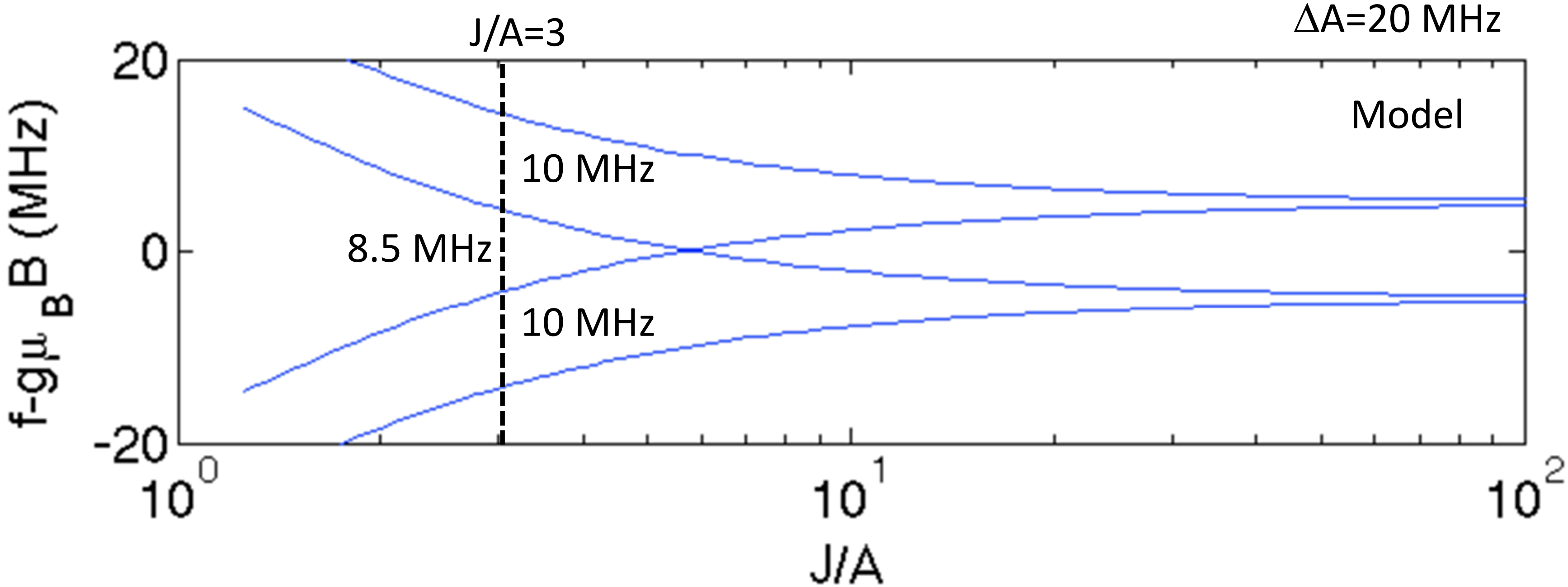

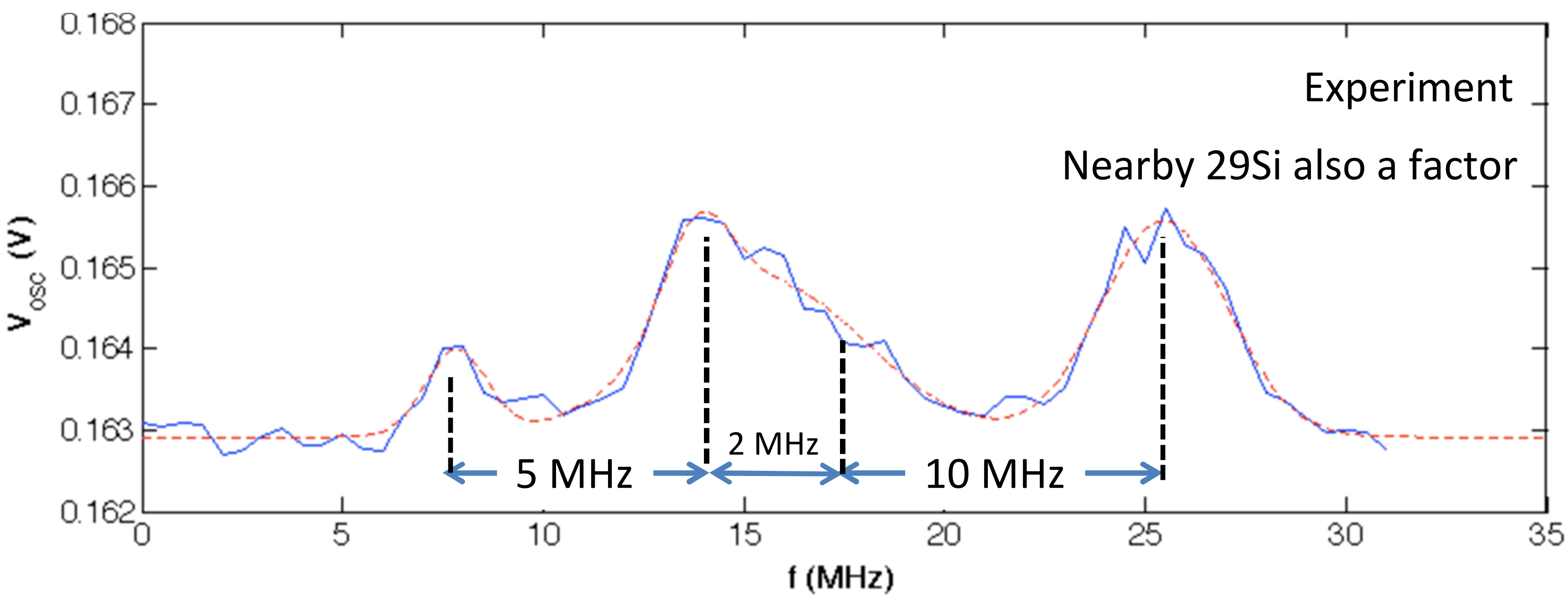

High Frequency Lines

D. R. Luhman, M. P. Lilly

Is this correct?

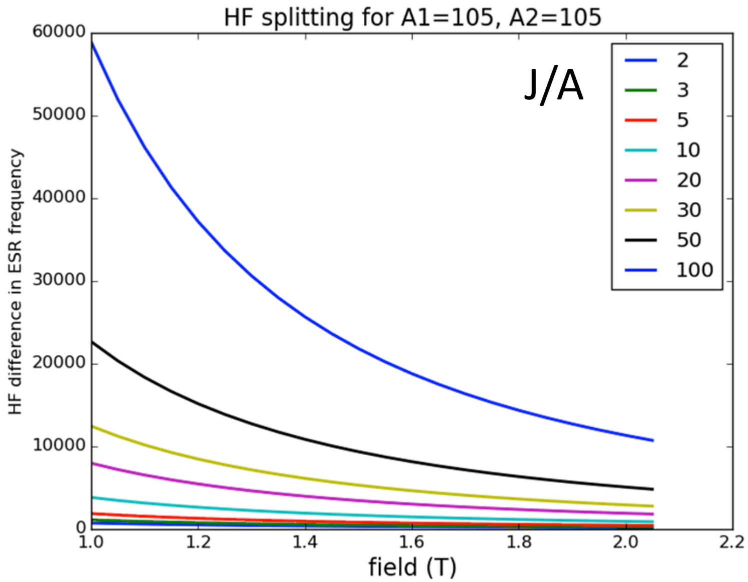

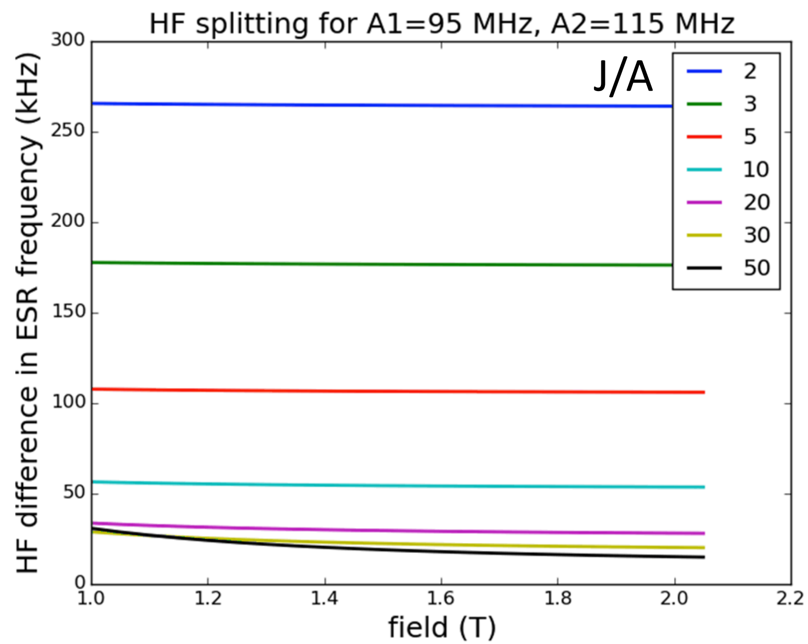

ΔA=14-24 MHz
J/A~2.5-4
Δf~165 kHz and independent of B

Consistent with Experiment

RF Reflectometry

Measure reflection off of load Z_L

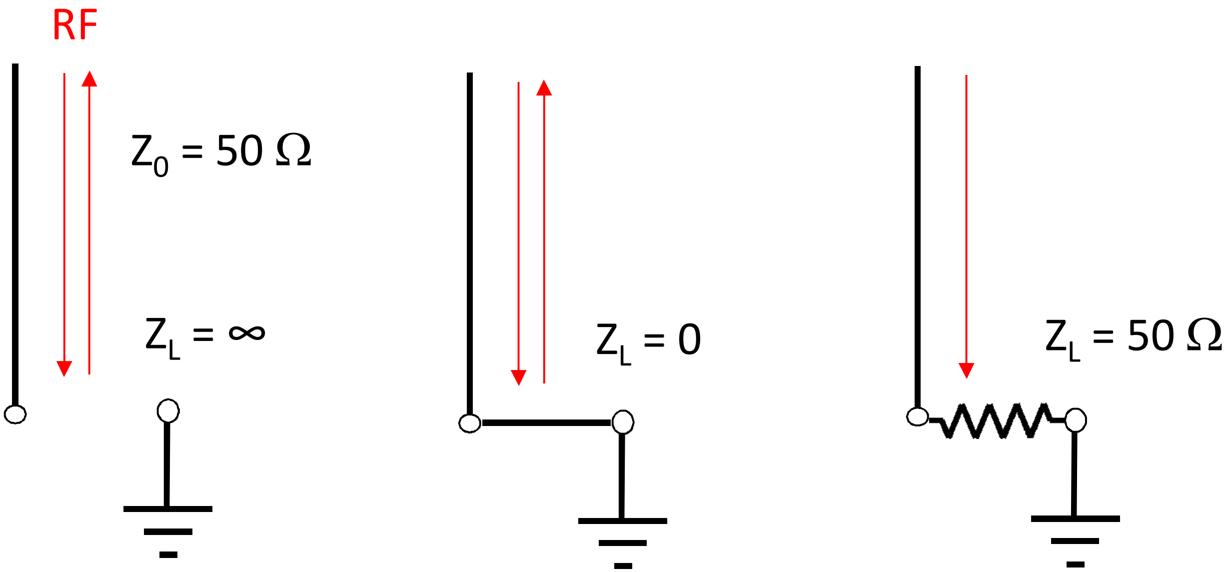

- Device Z ≠ 50 Ω – match impedance Z_L to transmission line Z_0

tank circuit:

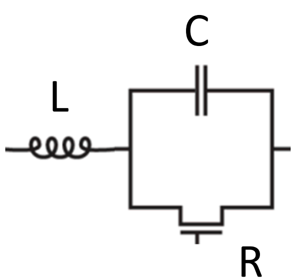

$Z_L \rightarrow 50\ \Omega$ for $2\pi f \sim 1/\sqrt{LC}$

Schoelkopf et al., Science 1998

Sandia National Laboratories

Reflectometry Circuit

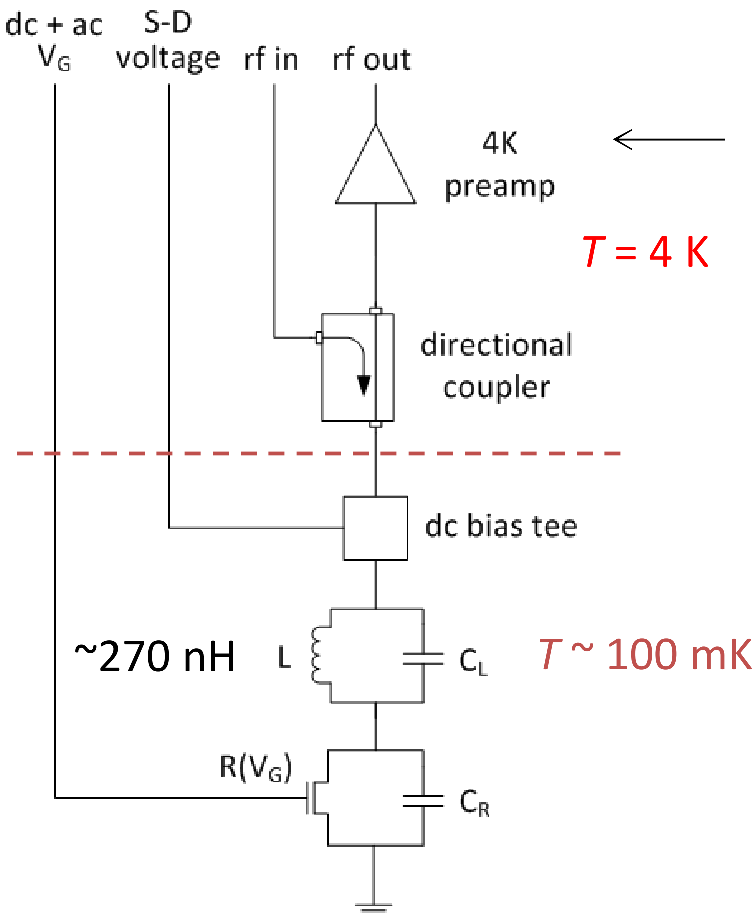

Quinstar HEMT amplifier (gain ~ 45 dB @ 300 to 420 MHz, T_N ~ 3 - 6 K)

RF DQD Platform

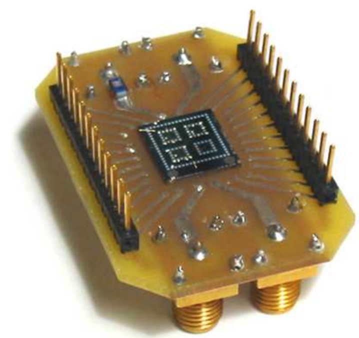

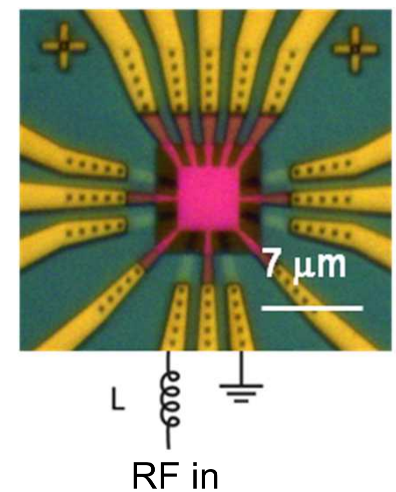

Tank Circuit Resonance vs. R_{device}

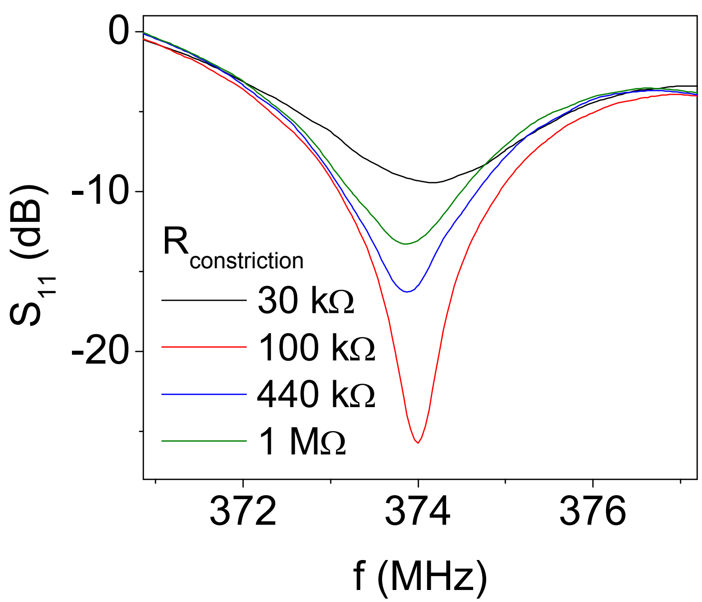

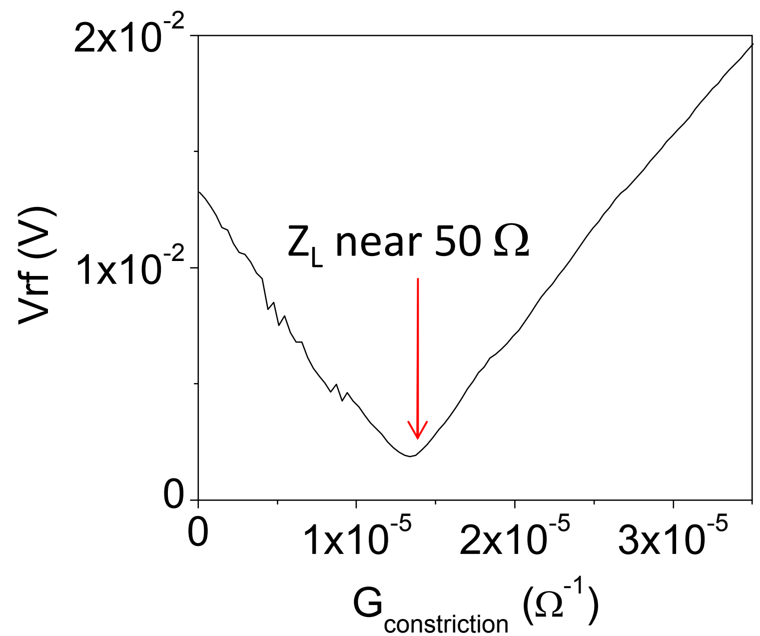

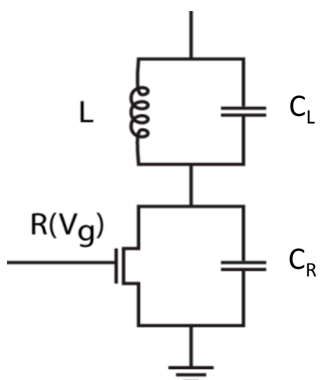

- Extract stray capacitances: C_L ~ 0.48 pF, C_R ~ 0.19 pF

Coulomb Diamonds: Quasi-dc vs. Reflectometry

<u>quasi-dc</u>

1 s/pt.

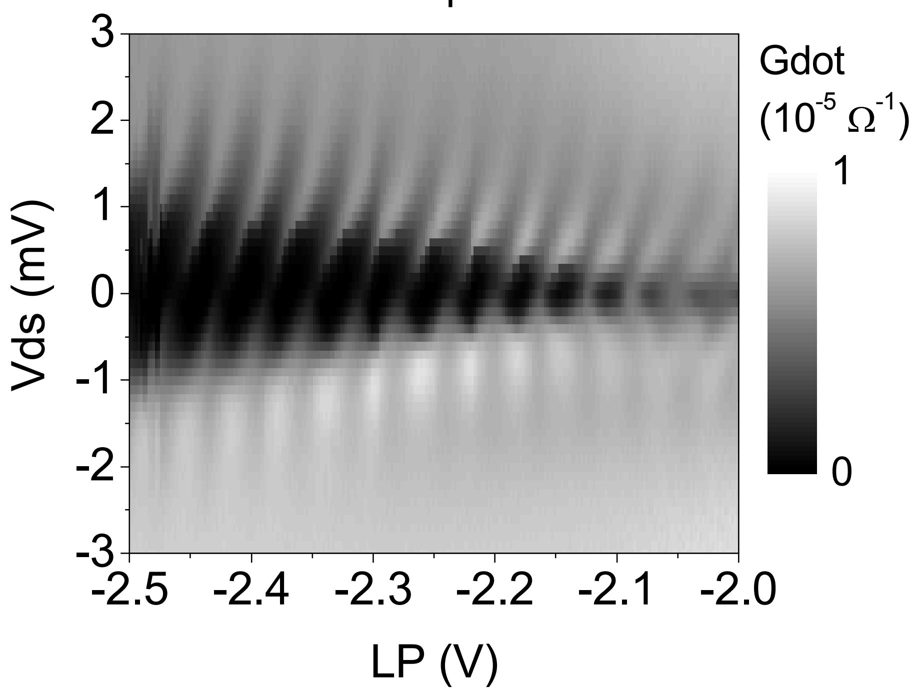

<u>reflectometry</u>

100 μs/pt., 16x avg.
2.5 mV rms on LP @100kHz

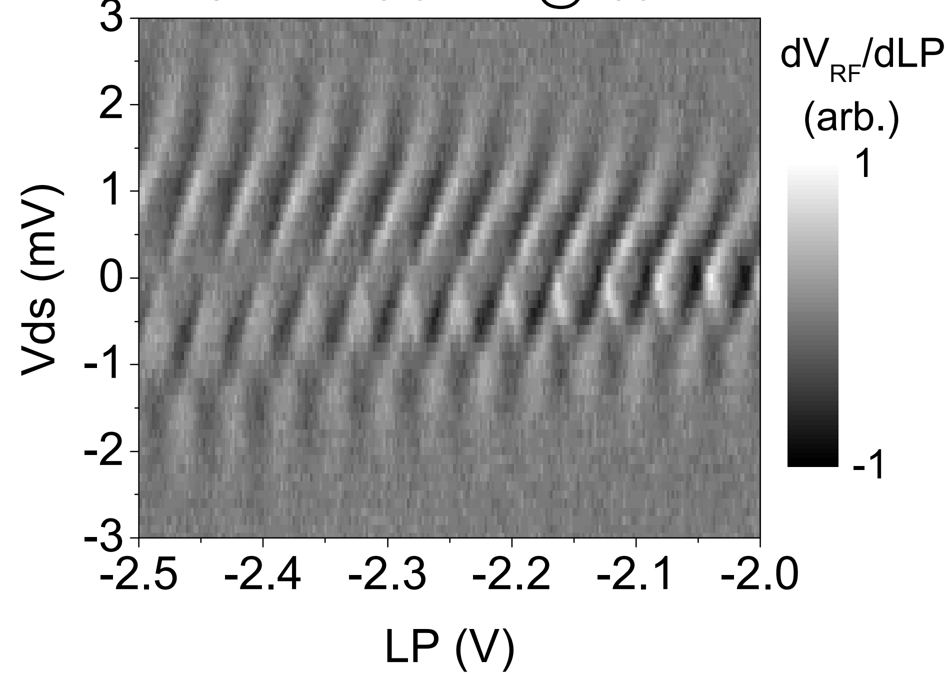

RF SET Bandwidth and Sensitivity

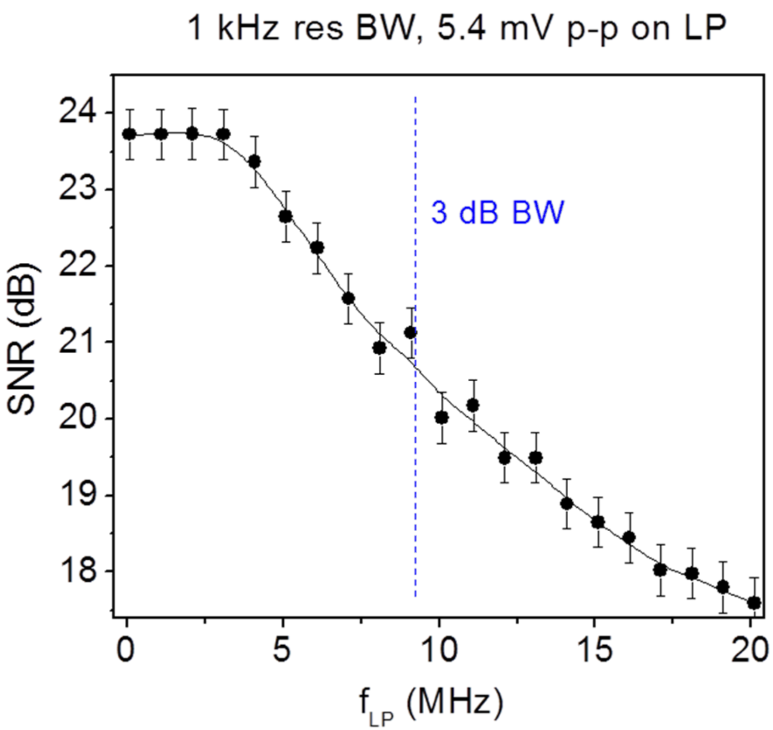

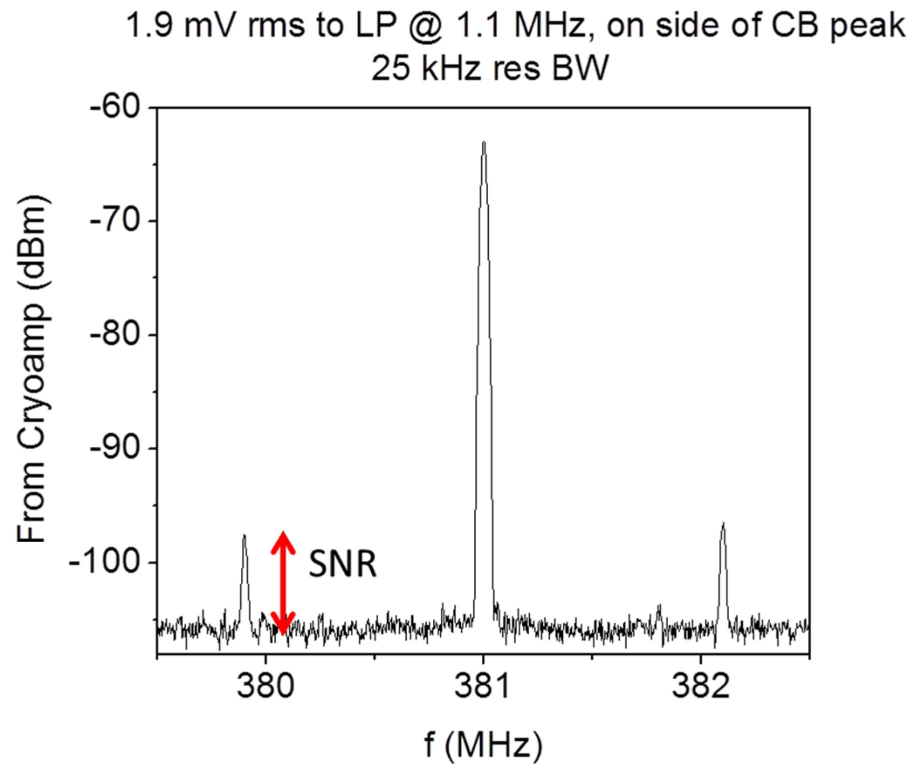

- Si MOS RF SET: 10 MHz BW and ~10^{-9} Ω^{-1} /√Hz sensitivity and for Vsd ~ 200 μV
- Corresponds to noise ~200 fA $Hz^{-1/2}$
- Other groups have achieved ~100 fA $Hz^{-1/2}$ (Reilley *et al.*, Phys. Rev. Lett. (2007)